predictive mineral discovery
COOPERATIVE RESEARCH CENTRE

pmd*CRC

Final Report

Micrometallogeny of Hydrothermal Fluids

Project F3

Compiled by: Tim Baker

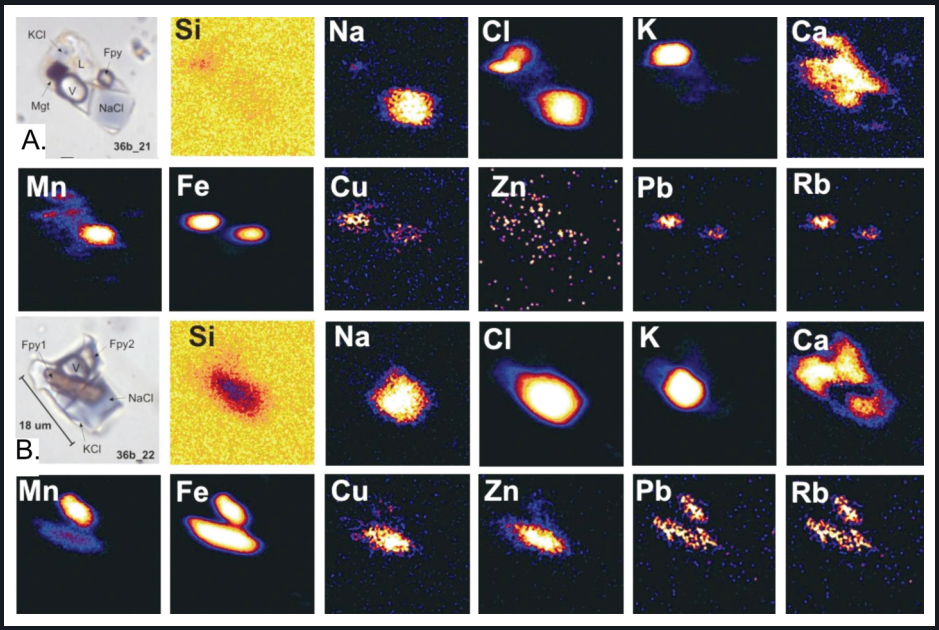

(a) and (b) type 1 multi-solid fluid inclusions associated with pre to syn-mineralisation stages at Osborne Cu-Au deposit. Fpy = ferropyrosmalite, NaCl = Halite, KCl = Sylvite, Cal = Calcite, Mgt = Magnetite.

CSIRO
AMIRA INTERNATIONAL
Australian Government
Geoscience Australia
MONASH University
THE UNIVERSITY OF MELBOURNE
JCU James Cook University
THE UNIVERSITY OF WESTERN AUSTRALIA

F3: Micrometallogeny of Hydrothermal Fluids

Final Report

February 2006

Compiled by:

Tim Baker
F3 Project Leader, Predictive Mineral Discovery CRC
Economic Geology Research Unit
School of Earth Sciences
James Cook University
Townsville 4811
Queensland
Australia
Ph: 07-47814756
Email: Timothy.Baker@jcu.edu.au

With contributions from:

Martina Bertelli, James Cleverley, Louise Fisher, Bin Fu, David Gillen, Wade Hodgson, Julie Hunt, Mark Kendrick, Geordie Mark, Terry Mernagh, Roger Mustard, Nick Oliver, Chris Ryan, Thomas Ulrich, and Patrick Williams

Table of Contents

Executive Summary

Distinct differences between hydrothermal fluids that formed barren to weakly mineralized regional alteration systems and iron oxide-copper-gold (IOCG) deposits have been recognized in Proterozoic IOCG districts. These differences include:

- Ultrasaline, multisolid inclusions are abundant in IOCG deposits but are mostly absent in regional alteration systems.
- Br/Cl ratios from PIXE analysis of individual fluid inclusions suggest that fluid salinity in the IOCG deposits was derived from halite dissolution and magmatic sources whereas regional fluids are characterized by higher Br/Cl ratios consistent with a bittern brine origin. These results are consistent with step-heating measurements of halogens using bulk inclusion techniques.
- Noble gas analyses also identify a magmatic/mantle fluid component in the IOCG deposits in addition to surface derived fluids that experienced crustal residence. There is no evidence for a magmatic/mantle fluid in the regional alteration systems.

Fluid mixing is interpreted to be a critical process in IOCG ore deposition. A combination of data suggests that major IOCG deposits formed by the mixing of the evaporite-related brines with a pulse of Cu-rich ultrasaline magmatic fluid. Evidence supporting this mixing model includes:

- Fluid inclusions in IOCG deposits display very wide ranges in salinity and temperatures. Different fluid inclusion types occur in the same paragenetic stages but there is an overall decrease in salinity through pre-, to syn- and post-ore stages.
- The most Cu-rich fluid inclusions occur in magmatic settings and have Br/Cl ratios consistent with a magmatic source. The most Cu-rich fluids in IOCG deposits also have Br/Cl ratios consistent with magmatic fluids.
- Br/Cl and Cu PIXE analyses of fluid inclusions in all settings suggest mixing between Cu-rich magmatic fluids and Cu-poor evaporite derived fluids.
- The largest IOCG deposit, Ernest Henry, has the strongest magmatic/mantle-like noble gas signature further suggesting a key role for magmatic fluids.

Exploration implications include:

- Terrane-scale - regions that contain evidence for both evaporitic and magmatic fluid reservoirs are most prospective.
- District to deposit-scale – the most prospective systems will contain evidence for ultrasaline magmatic fluids and also fluid inclusions with a wide range of salinities and temperatures.

1.0 Introduction

This report is a synopsis of research compiled and carried out within the Predictive Mineral Discovery CRC F3 project "Micrometallogeny of hydrothermal fluids". The F3 project's original objectives were:

1. Geology-driven terrane and ore fluids investigations: this was the main focus of the project and was conceptually designed to evaluate the chemistry and fluid processes within mineral systems in order to extend the focus of fluid studies beyond direct ore deposit analysis (Fig. 1). In particular this approach was applied to iron oxide-copper-gold (IOCG) systems in the Cloncurry district and this is the main focus of the synopsis presented here (Fig. 2). In addition work was also carried out on Proterozoic IOCG systems in the Wernecke Mountains, Canada, in order to compare a well mineralized district (Cloncurry) with a region that contains numerous IOCG occurrences but no major IOCG deposits (Hunt et al., 2005; Gillen et al., 2004, 2005). Additional fluid inclusion studies were carried out on Broken Hill Type deposits in the Cloncurry region (Williams et al., 2005). The F3 research project also contributed to fluid inclusion studies in the Y3 Yilgarn project and the I4 Mount Isa copper project, and has developed strong research collaboration with the H4 project.

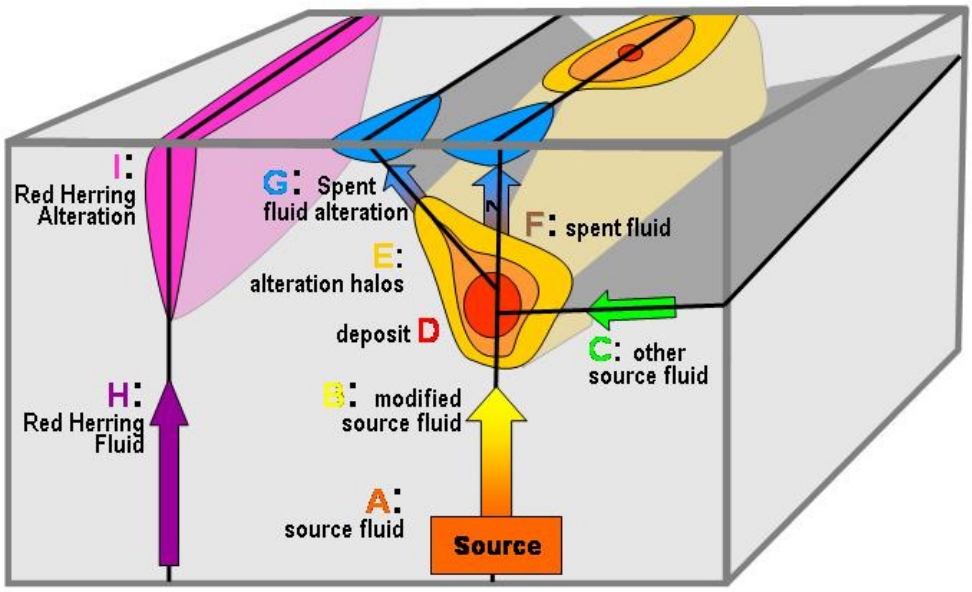

Figure 1: Conceptual F3 project model.

2. LAICPMS and PIXE technique and methodology development: these two techniques were utilized throughout the project and methodologies were developed for their combined application. These results are reported in Baker (2003), Williams et al. (2004a), and Bertelli et al. (2006).

3. Diamond-cell autoclave experiments: this component of the project was a scoping-collaboration in year one of F3 with Joel Brugger at the Museum of South Australia and subsequently developed into an ARC project outside the scope of F3. No results are reported from this research.

4. Database development and fusion with numerical modelling: development of a web-based database for fluid inclusion research has been successful and is currently accessed at http://www.ga.gov.au/minerals/research/methodology/geofluids/flincs_about.jsp. Further development of this work is being carried out elsewhere in the CRC through separate modeling and database projects. The F3 project has carried out integration of fluid inclusion chemistry and chemical modeling and these results are reported by Bertelli et al. (2004, 2006).

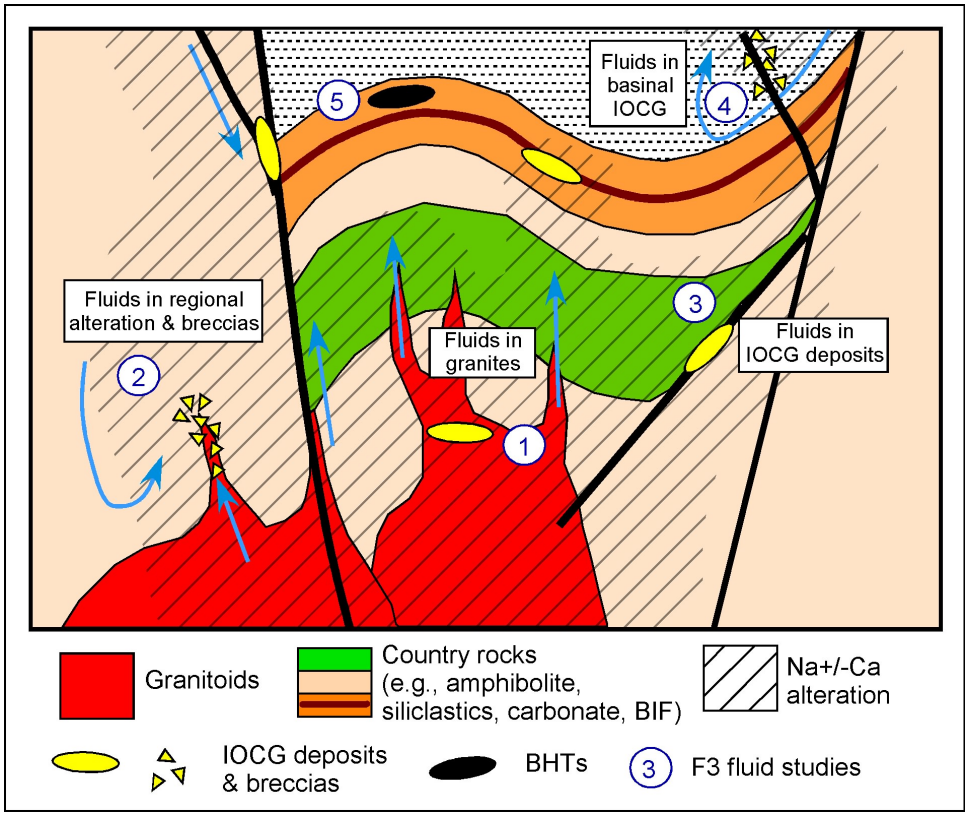

Figure 2: Model depicting the setting of hydrothermal systems studied in the F3 project with an emphasis on IOCG environments.

2.0 Comparison of Fluid Inclusions associated with IOCG Deposits, Barren Regional Alteration Systems and Granites in the Cloncurry District

2.1 Geological Setting and Fluid Inclusion Characteristics of IOCG Deposits

Previous selected fluid inclusion studies of Cloncurry IOCG deposits are summarized in Table 1 and includes data from Osborne, Starra, Eloise and Mount Dore. The main focus of IOCG deposit-based research within the F3 project was Osborne and Starra (Fig. 3; Baker, 2003; Mustard et al., 2004), and further work on these deposits is continuing through Louise Fisher's PhD research (Fisher, 2005).

Geology of IOCG Deposit

The Osborne deposit (11.3 Mt @ 2.9% Cu, 1.18 g/t Au; Adshead et al, 1998) is hosted within a multiply deformed sequence of upper amphibolite facies metamorphic rocks, including feldspathic psammites, pelites, metasedimentary gneisses, amphibolites, and pegmatites of the Mount Isa Eastern Sucession. Mineralization can be divided into the 'Western' and 'Eastern' domains based on differences in the host rocks and mineralization characteristics. The western domain contains the bulk of the Cu-Au mineralization, occurs at the contact between a banded ironstone formation and feldspathic psammite, and is dominated by a hematite-magnetite-pyrite mineral assemblage. The eastern domain mineralization is not spatially associated with the ironstones, forms a discrete body hosted within strongly silicified rocks, and exhibits a more reduced pyrrhotite-magnetite±pyrite assemblage. Ages obtained from various minerals within the deposit indicate a complex hydrothermal history. U-Pb analyses on titanite from sodic-calcic alteration have an age of 1595 Ma consistent with Ar-Ar ages from hornblende in foliated alibitized rocks (Perkins and Wyborn, 1998; Rubenach et al., 2001; Gauthier et al., 2001). Two Re-Os ages on molybdenite-bearing ore samples are also consistent with a 1595 Ma age (Gauthier et al., 2001) whereas mineralization-related hornblende and biotite have younger ages at ~1540 Ma (Perkin and Wyborn, 1998).

The Starra orebodies (6.9 Mt @ 1.7% Cu; 4.8 g/t Au) also occur in magnetite-hematite ironstones within albite and magnetite-biotite rich alteration that replaced schist and calc-silicate host rocks (Rotherham, 1997; Rotherham et al., 1998). The alteration and ore occurred late in the deformation history of the region during fabric intensification in a steeply dipping shear zone. The Au-Cu ore is dominantly confined to the ironstones and occurs in seven discrete zones over 5.5 km of strike. Pyrite, chalcopyrite, anhydrite, barite, calcite, and gold, locally with bornite and chalcocite, were precipitated from late oxidizing fluids in association with brecciation and hematization of the magnetite host (Rotherham 1997). Perkins and Wyborn (1998) reported a 1503 Ma age from mineralization related biotite at Starra.

The Eloise deposit (3.1 Mt @ 5.5% Cu; 1.4 g/t Au) is also localized by a steep shear zone and distinguished by a pronounced mineral zoning with the economic lodes separated from the main concentrations of magnetite by several hundred metres (Baker, 1998). The lodes are hosted by amphibolite facies meta-arkoses and characterized by early albitization overprinted by high temperature hornblende-biotite ± quartz alteration which was selectively replaced by pyrrhotite and chalcopyrite during mineralization. Ore formation was accompanied by the development of a lower temperature alteration

paragenesis containing actinolite, chlorite, muscovite and carbonate. Baker et al. (2001) used ^{40}Ar-^{39}Ar dating of hornblende to constrain the age of the mineralization to ~1530 Ma.

The Mount Dore copper deposit (inferred resource 26Mt @ 1.1% Cu) occurs within steeply east-dipping quartz-muscovite schists and carbonaceous slates of the Staveley Formation structurally overlying metacalcarenites, marbles and metabasalts (Beardsmore, 1992). Mount Dore displays a complex history of brecciation and alteration related to movement along the Mount Dore Fault Zone and associated hydrothermal activity. Early alteration produced K-feldspar (or biotite), tourmaline, sericite and quartz. Later alteration produced carbonate (dolomite and calcite), apatite and chlorite. All phases are associated with all brecciation styles, but the most pervasive alteration is associated with the intensively milled breccias. Sulphide mineralization is associated temporally with carbonate alteration, and comprises pyrite and chalcopyrite, with minor sphalerite and galena.

IOCG Fluid Inclusions

Fluid inclusions in Cloncurry IOCG deposits can be classified into four main fluid inclusion types (Table 1), although in detail fluid inclusions in each deposit have been classified more complexly (e.g., Baker, 1998; Rotherham et al., 1998; Williams et al., 2001).

Deposit	Type	Phases	Abundance	Th (C)	Salinity*	P (kbars)	References
Eloise	1	L+V+nS	Abundant	157 to 544	30 to 60	1 to 3.5	Baker, 1998
	2	L+V+S	Common	123 to 560	28 to 54		
	3	L+V	Common	101 to 192	4 to 36		
	4	CO2-H2O	Rare	?	?		
Osborne	1	L+V(+/-CH4)+nS	Abundant	141 to 544	30 to 80	1.8 to 4	Adshead, 1996
	2	L+V+S	Common	132 to 265	29 to 36		
	3	L+V	Common	98 to 196	0.4 to 25		
	4	CO2+/-CH4	Common	-11.8 to 29	?		
Starra	1	L+V+nS	Abundant	225 to 615	30 to 52	2.1 to 3.7	Rotherham, 1997
	2	L+V+S	Abundant	110 to 345	27 to 38		
	3	L+V	Abundant	127 to 154	8 to 15		
	4	CO2+/-CH4	Common	-20.2 to 24			
Mount Dore	1	L+V+nS	Abundant	430 to 530	48 to 55		Beardsmore, 1992
	2	L+V+S	Abundant	145 to 550	29 to 36		
	3	L+V	Abundant	97 to 253	1 to 15		
	4	CO2+/-H2O	Rare	?	?		
	5	V+L	Common	208 to 392	?		

Table 1: Summary of fluid inclusion characteristics from IOCG deposits in the Cloncurry district. *NaCl wt % equiv.

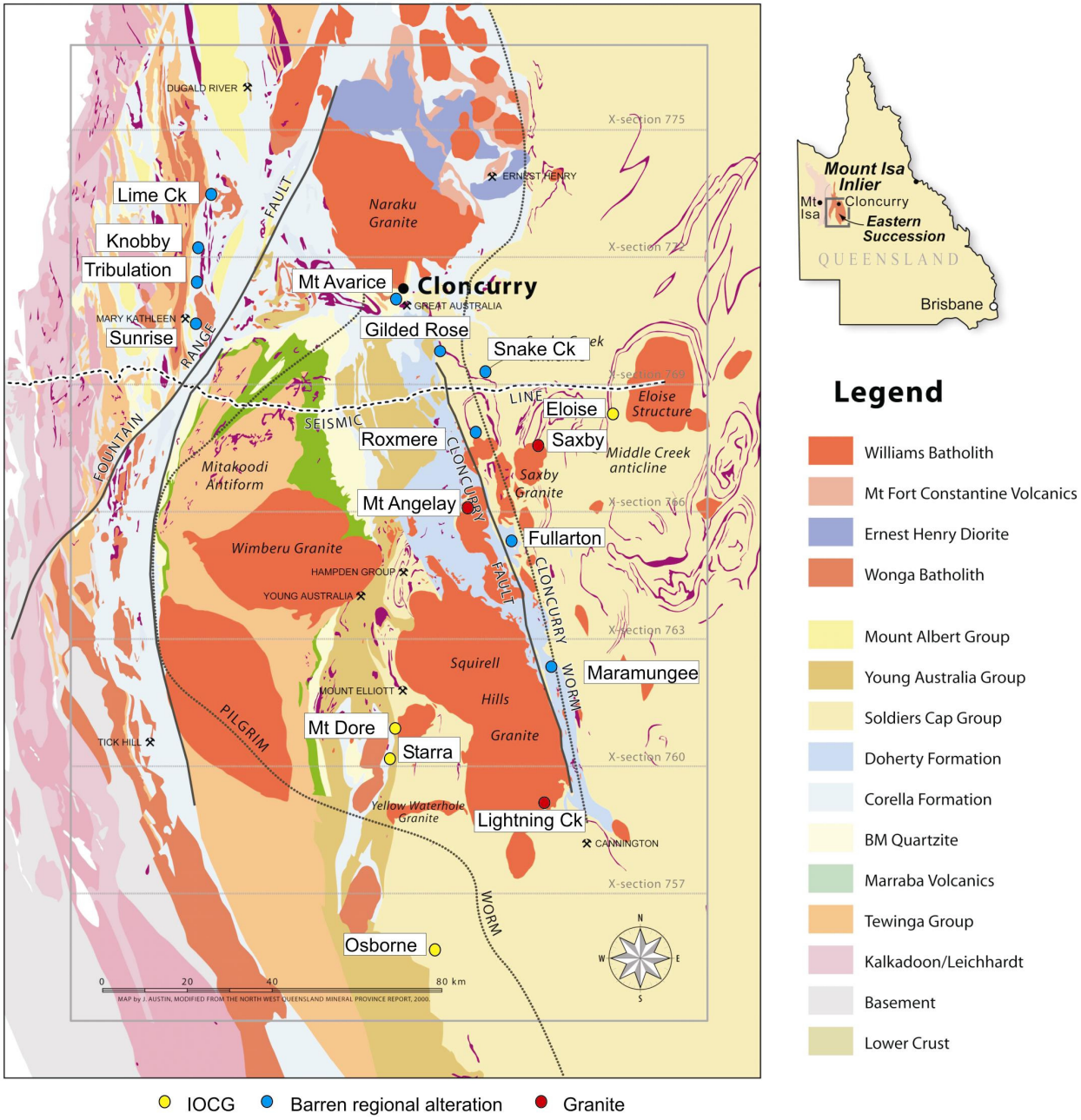

Figure 3: Basement geology map (including undercover interpretations) of the Mount Isa region compiled by I2-3 researchers. Coloured dots represent F3 study areas and locations from which previous fluid inclusion data has been compiled including IOCG deposits (yellow), barren regional alteration systems (blue) and granite-hosted environments (red).

The main fluid inclusion types are:

- Type 1 multisolid inclusions (L+V+nS where n > 1) contain halite in addition to one or more solid phases including sylvite, ferropyrosmalite, iron and/or manganese chloride, carbonate, magnetite, barite, anhydrite, barium chloride, and rare chalcopyrite. In all the deposits referred to here these fluid inclusions are abundant and occur in pre- and syn-ore stage veins. Salinity estimates from microthermometric studies range from 30 to >60 wt. % total salts and homogenization temperatures have a large range typically between ~200 and 550 ºC (Table 1 and Figs. 5 and 6). In the majority of inclusions homogenization occurs via daughter phase dissolution.
- Type 2 halite-bearing (L+V+S where S = halite) inclusions commonly occur syn to post-ore. Homogenization temperatures typically range between 120 and 350ºC (however some homogenization temperatures are recorded up to 550 ºC) and salinity estimates range mostly between ~30 to 40 wt. % NaCl equiv. (locally up to 55 wt. % NaCl equiv.; Figs. 5 and 6). In the majority of inclusions homogenization occurs via halite dissolution.
- Type 3 two phase aqueous inclusions (L+V) are generally secondary and post-date ore. The vapour bubble occupies < 10 % of the volume of the inclusion. Homogenization temperatures range from ~100 to 250 ºC and have low to moderate salinity estimates (~1 to 36 wt. % NaCl equiv.).
- Type 4 carbonic inclusions ($CO_2 \pm H_2O \pm CH_4 \pm N_2$) have variable abundance from being rare at Eloise and Mount Dore to common in Osborne and Starra. They generally contain a CO_2-phase that homogenizes via CO_2-vapour bubble disappearance (e.g., Osborne and Starra; Table 1). In some cases a thin rim of water is present, and at Osborne halite ± other daughter phases occur that likely represent heterogeneous entrapment during fluid unmixing or mixing (see below; Mustard et al., 2004; Fisher, 2005). Laser Raman studies have locally identified CH_4 and N_2.

The timing relationships and microthermometric behaviour of the different fluid inclusion types are important to constrain when interpreting processes from fluid inclusion data. All four IOCG data sets compiled in this review show very large ranges in salinity and homogenization temperature between types 1, 2 and 3 inclusions. Type 1 multisolid inclusions are pre- to syn-ore and may occur with type 2 halite-bearing inclusions (Fig. 7a). Type 3 two phase aqueous inclusions are for the most part post-ore but also commonly occur with some type 2 inclusions (Fig. 7b). Therefore, the aqueous-salt fluid inclusions in the IOCG deposits have a distinct paragenesis from pre- to syn-ore type 1 multisolid inclusions with high homogenization temperatures and ultra-high salinity, to syn- to post-ore, type 2 halite-bearing inclusions with moderate homogenization temperatures and moderate to high salinity, through to late, mostly post-ore lower salinity, low homogenization temperature type 3 two phase aqueous fluid inclusions. This consistent fluid inclusion paragenesis observed in the deposits described represents a major decrease in salinity from pre- to post ore stages that is consistent with fluid mixing.

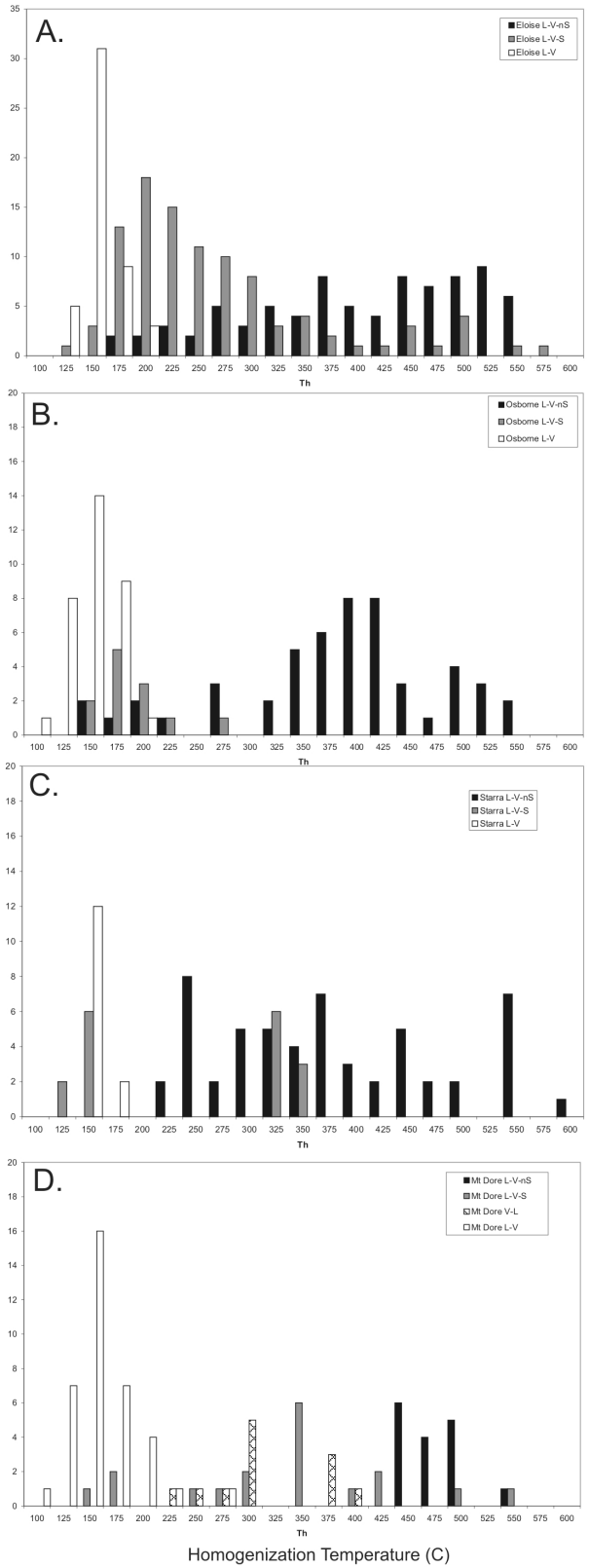

Figure 5: Homogenization temperature histogram for Cloncurry IOCG deposits.

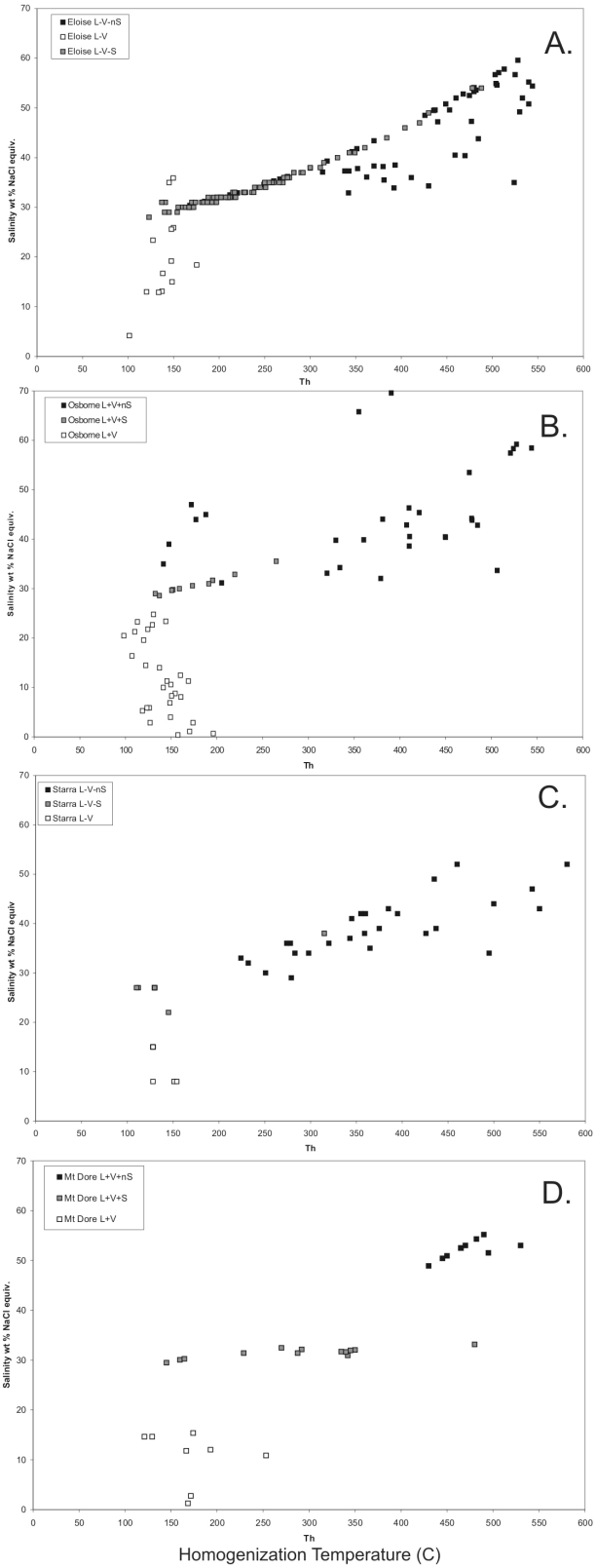

Figure 6: Homogenization temperature versus salinity scatter plot for Cloncurry IOCG deposits.

There is also evidence from all four deposits that type 4 carbonic inclusions occur in the same trails and clusters as type 1 multisolid inclusions (Fig. 7c and d) which has lead several researchers to interpret these relationships as a result of fluid unmixing (Beardsmore, 1992; Adshead, 1995; Pollard, 2000;

Mustard et al., 2004). One of the arguments against fluid unmixing is the fact that the vast majority of type 1 inclusions homogenize via daughter phase dissolution with the vapour phase typically disappearing at temperatures < 300 ºC. Under immiscible conditions the vapour bubble will be the last phase to disappear (Bodnar, 1995). Fluid mixing would be an alternative mechanism for the textural relationships and phase behaviour observed, or alternatively post-entrapment processes such as hydrogen diffusion, fluid-mineral reaction or metastable homogenization behaviour may have resulted solid phases melting last in the type 1 inclusions.

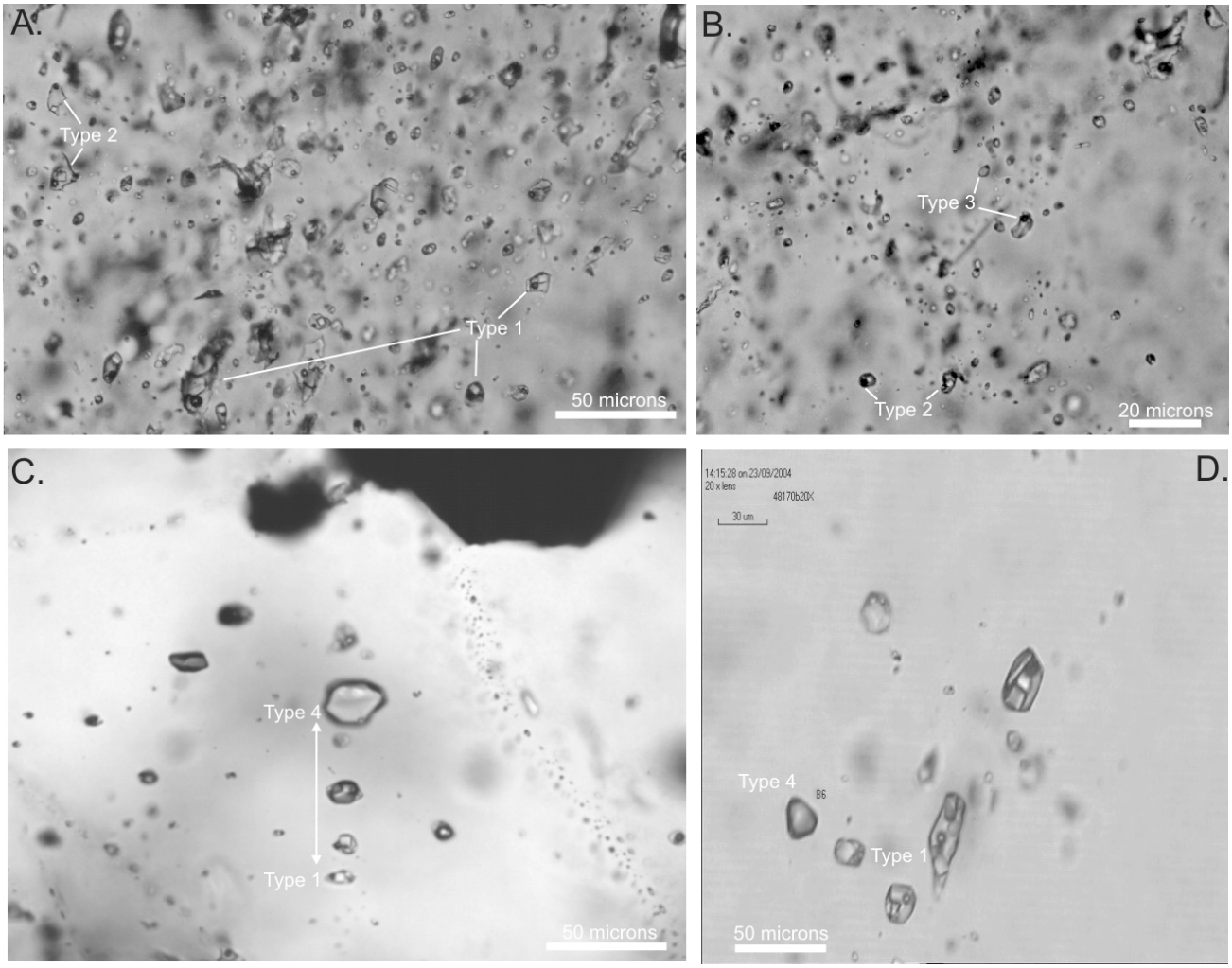

Figure 7: a. Mixed populations of type 1 multisolid and type 2 halite-bearing fluid inclusions from the Eloise deposit. b. Mixed populations of type 2 halite-bearing and type 3 two phase aqueous fluid inclusions from the Eloise deposit. c. A trail of type 4 carbonic inclusions and type 1 multisolid inclusions with heterogeneous mixtures of salt, water and carbon dioxide in inclusions between the end-members. This relationship may reflect mixing or unmixing (from Osborne; Mustard et al., 2004). d. Type 1 multisolid inclusions and a rare type 4 inclusion from the Eloise deposit.

2.2 Geological Setting and Fluid Inclusion Characteristics of Barren Regional Alteration Systems

Geology of Barren Regional Alteration

Fluid inclusion research on barren regional alteration systems includes past studies by De Jong and Williams (1995), Xu (2000), Hodgson (unpublished) and F3 research by Fu et al. (2004a and b) and Martina Bertelli's ongoing PhD research (Fig. 3). De Jong and Williams (1995) presented research from geological sections mapped through intensely altered breccias in the Fullarton River and Maramungee Creek areas of the Cloncurry district. These rivers are oriented perpendicular to the main structural grain and cut through structurally controlled sodic-calcic alteration and associated brecciation that affected at least 200 square kilometres along the Cloncurry fault at the contact between the Soldiers Cap group and the Doherty Formation. The penetrative N-S S_2 foliation in these rocks is overprinted by intense albite-actinolite±magnetite±titanite+diopside alteration. K-feldspar-quartz-hematite and epidote-prehnite-calcite-quartz assemblages overprint the earlier sodic-calcic alteration and late stage comb quartz veins are controlled in fractures related to late movement on the Cloncurry fault. The timing of the latter event is unknown and may be unrelated to the main regional alteration systems. Fu et al. (2004a and b) studied fluid inclusions in veins and host rocks related to albitisation from Knobby, Tribulation, Lime Creek and Sunrise in the Mary Kathleen Fold Belt and from Mt Avarice, Roxmere-Marimo, Snake Creek and Gilded Rose in the Cloncurry district (Fig. 8a and b). This work built upon previous fluid inclusion studies by Wade Hodgson (unpublished). All samples were collected either from quartz-calcite-pyroxene±amphibole veins associated with albitisation in the metamorphosed calc-silicate and dolerite wall rocks or from breccias in the Mary Kathleen Group (Corella type) and Soldier's Cap Group (Gilded Rose type), which contain quartz clasts. Red hematite-K-feldspar alteration commonly occurs in the Gilded Rose breccias. Martina Bertelli's ongoing research has focused on barren breccia systems at the northern tip of the Williams batholith near the Roxmere station (Fig. 3). Sodic-calcic alteration and brecciation contains clasts of granite pegmatites with granophyric and unidirectional solidification textures indicative of fractionated and volatile-rich granite roof zones. The clasts are altered by micro-fracture controlled albitization (Fig. 8c, d and e).

Barren Regional Alteration Fluid Inclusions

Fluid inclusions documented in the three studies have many similarities (Table 2). Type 1 multisolid inclusions common to the ore deposits are mostly absent from the barren regional alteration systems (Fig. 9). Type 2 halite-bearing inclusions and type 3 two phase aqueous inclusions are the most abundant inclusion types in addition to locally common type 4 carbonic inclusions. De Jong and Williams (1995) identified type 2 and 3 inclusions that have moderate to high salinities (~12 to 40 wt. % NaCl equiv.) and high Ca:Na ratios. Homogenization temperatures mostly range between 100 and 300 ºC (Figs. 9a to d). Similar salinity and homogenization temperatures are recorded from type 2 and 3 inclusions from barren breccia system near the northern tip of the Williams batholith (Fig. 9e and f).

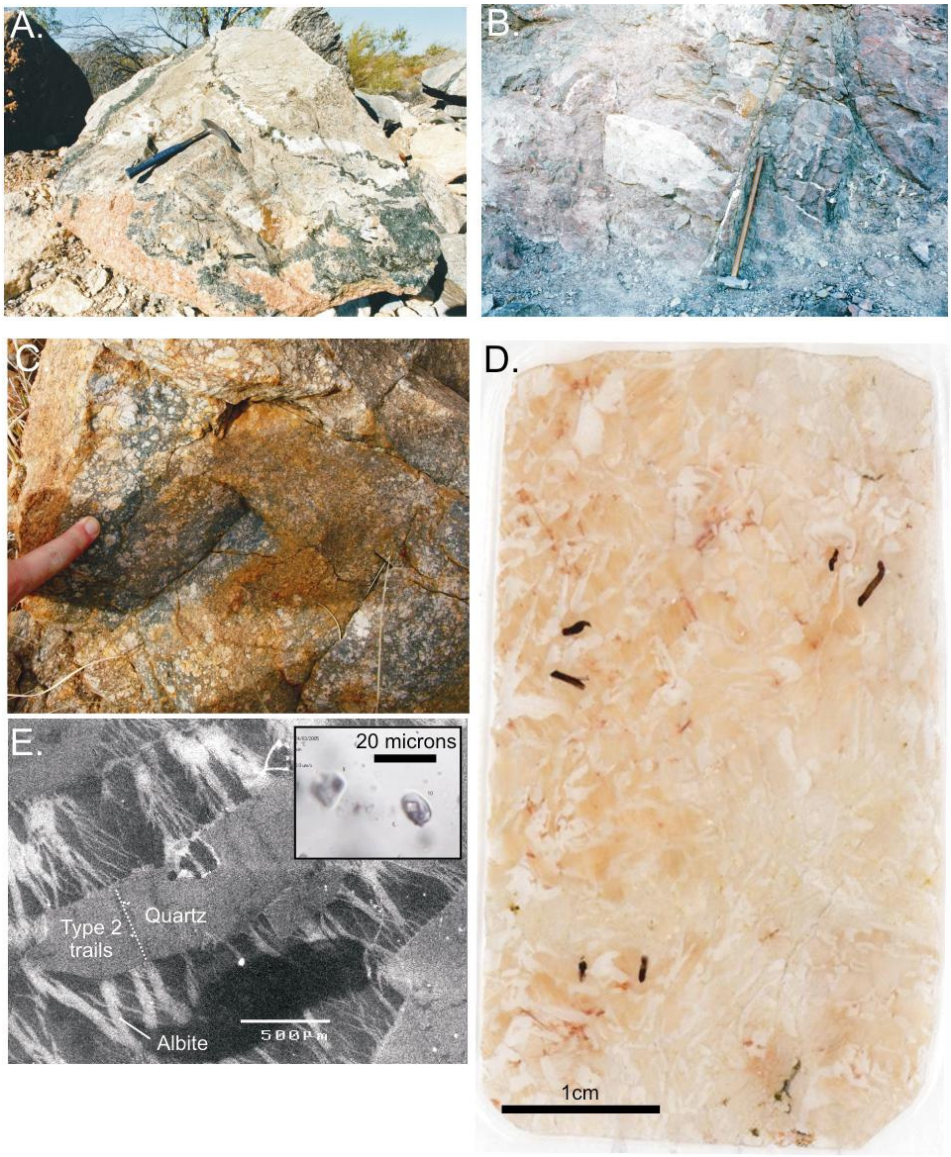

Figure 8: Barren regional albitization at (a) Knobby and (b) Mount Avarice (Fu et al., 2004a and b). c. Barren albitized breccia on the margins of the northern tip of the Williams batholith. d. Thin section from clast of granophyric textured granite from the breccia pipe shown in (c). e. Cathode luminescence image of (d) showing late albitization along fractures with related fluid inclusions (type 2 halite-bearing – see inset) in secondary trails within quartz. (c) to (e) courtesy of Martina Bertelli's ongoing PhD research.

Hodgson (unpublished) and Fu et al. (2004a and b) also document type 2 inclusions with salinity ranges between 30 and 40 wt % NaCl equiv. and homogenization temperatures between 170 and 300 ºC and rare type 1 inclusions with salinities of up to 60 wt % total salts and homogenization temperatures up to 550 ºC in various regional albite-altered localities (Table 2). Type 4 carbon dioxide inclusions have also been found in the barren breccia system near the northern tip of the Williams batholith by Bertelli. The CO_2 homogenization temperatures range between -17.5 and 30.5 ºC. Fu et al. (2004a and b) also report CO_2 inclusions (which locally have minor N_2) that have CO_2 homogenization temperatures between -37 and 30.2 ºC.

Area	Alteration	Type	Phases	Abundance	Th (C)	Salinity*	P (kbars)	References
Maramugee Creek & Fullarton River	Sodic-Calcic	2	L+V+S	Abundant	158 to 298	28 to 41	2 to 3	De Jong & Williams, 1995
		3	L+V	Common	137 to 266	23 to 30		
	K-feldspar	2	L+V+S	Rare	131 to 146	26 to 28		
		3	L+V	Common	123 to 216	12 to 28		
	Late comb quartz	2	L+V+S	Common	114 to 300	21 to 33		
		3	L+V	Common	55 to 184	20 to 28		
Roxmere breccia pipe	Sodic-Calcic	2	L+V+S	Abundant	168 to 360	30 to 43	?	Bertelli, unpub.
		3	L+V	Common	144 to 178	4 to 12		
		4	CO2	Common	-17.5 30.5	5 to 16		
Various locations in MKFB & Cloncurry	Sodic-Calcic	1	L+V+nS	Uncommon	200 to >550	30 to 60	2 to 3.5	Fu et al., 2003; 2004; Hodgson (unpublished)
		2	L+V+S	Abundant	116 to 500	27 to 52		
		3	L+V	Abundant	79 to 423	1 to 35		
		4	CO2	Common	-37 to 30.2			

Table 2: Summary of fluid inclusion characteristics from barren regional alteration systems in the Cloncurry district. *NaCl wt % equiv.

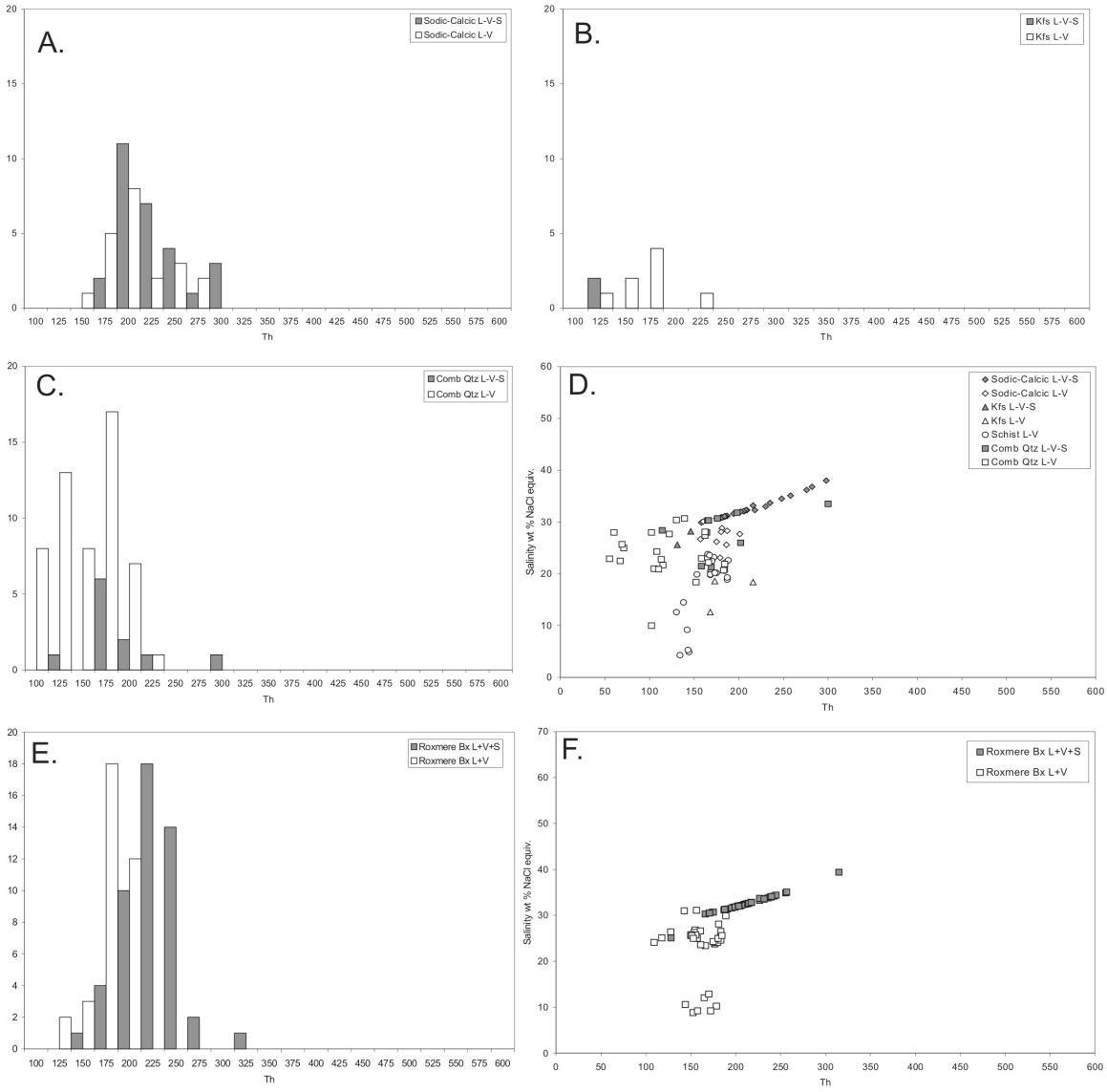

Figure 9a-f: Fluid inclusion homogenization temperature (Th) histograms and salinity versus Th scatter plots for barren regional albitization compiled from DeJong and Williams (1995), plots (a) to (d), and Martina Bertelli's ongoing PhD research in plots (e) and (f).

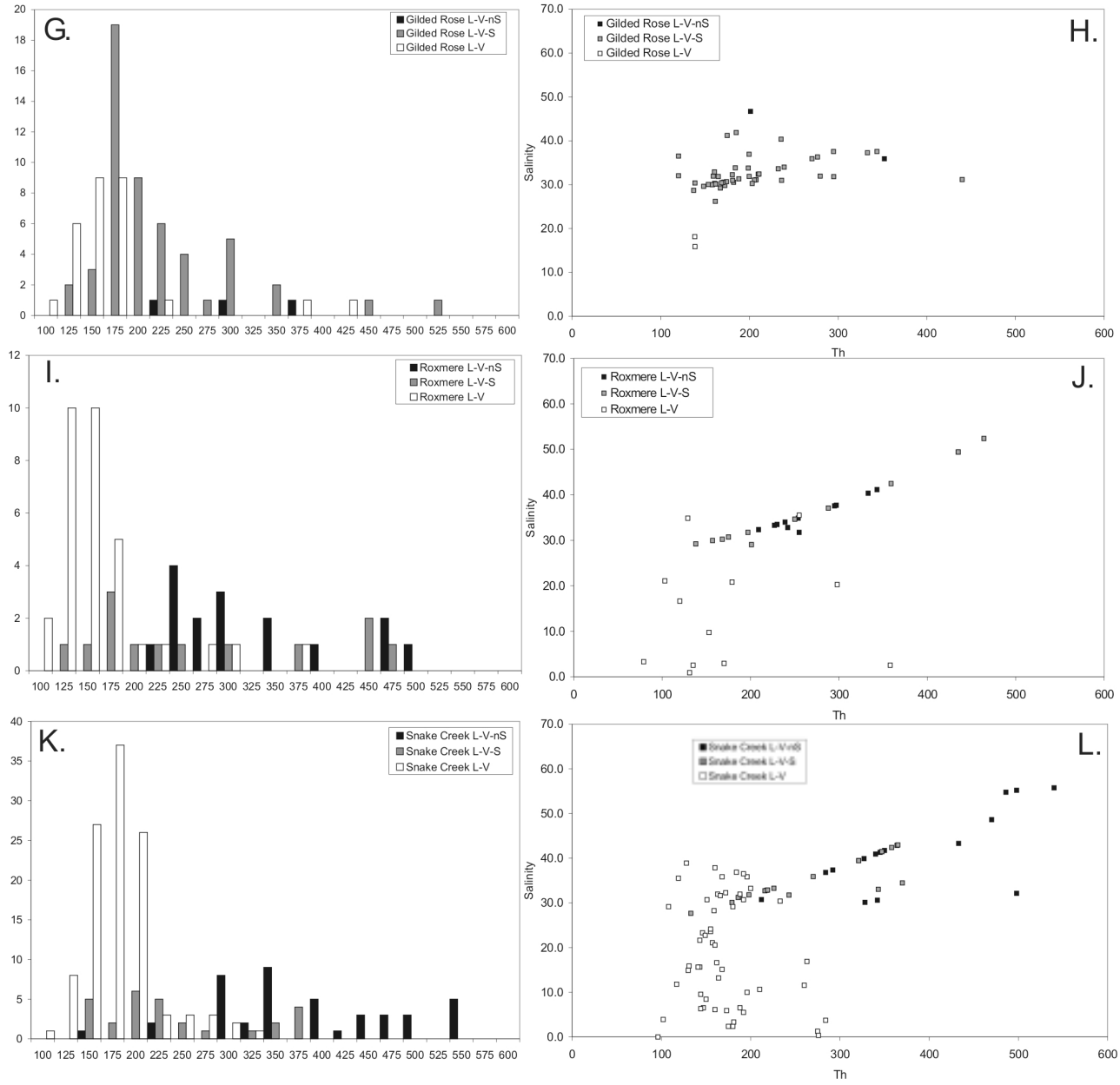

Figure 9g-l: Fluid inclusion homogenization temperature (Th) histograms and salinity versus Th scatter plots for barren regional albitization compiled from Wade Hodgson (unpublished) including (g) & (h) Gilded Rose, (i) & (j) Roxmere and (k) & (l) Snake Creek. The diagrams illustrate the abundance of type 2 halite-bearing and type 3 two-phase aqueous inclusions in the barren regional albitization, and lesser type 1 multi-solid inclusions.

2.3 Geological Setting and Fluid Inclusion Characteristics of Granite Hosted Magmatic-Hydrothermal Systems

Thorough fluid inclusion microthermometric data is still lacking from granite-hosted magmatic-hydrothermal systems in the Cloncurry district, however, there are several studies available for comparison with IOCG deposits and regional barren alteration. Perring et al. (2000) documented barren magnetite-rich magmatic-hydrothermal alteration systems at the Lightning Creek prospect. Within F3 Mark et al. (2004) studied fluid inclusions from the Mount Angelay Igneous Complex (MAIC) and Mustard et al. (2005) carried out LAICPMS studies on fluid inclusion from MAIC, Lightning Creek and the Saxby granite.

Geology of Granite Hosted Magmatic-Hydrothermal Systems

The Paleoproterozoic cover sequence rocks in the Cloncurry district were intruded by a series of syn- to post-peak metamorphic intrusions that form the Williams and Naraku Batholiths (mostly emplaced between 1550 and 1500 Ma). Intrusions of this age have an outcrop exposure >1500 km^2, and are predominantly potassic, although rare sodic intrusions of similar age do occur. The main K-rich phases of the batholiths were emplaced in an intracratonic environment and are largely composed of metaluminous, alkaline to subalkaline, magnetite-bearing granitoids that typically plot as 'A-type' on geochemical discrimination diagrams (Mark et al., 2004).

The granite-hosted Lightning Creek prospect lacks any significant Cu-Au mineralization but is characterized by a magnetite-rich vein system that has resulted in a 9000 nT magnetic dipole anomaly occupying some 6 km^2 (Perring et al., 2000). The host rocks consist largely of quartz monzodiorite and monzogranite both of which contain diorite enclaves. These rocks are cut by a set of subhorizontal texturally complex quartz-plagioclase-rich sills and associated magnetite veins that display a range of magmatic-hydrothermal transition textures (Fig. 10 a and b; Perring et al., 2000). The host rocks are partly altered to a plagioclase-diopside assemblage that retains a typical magmatic oxygen isotope composition and the whole package is believed to reflect magmatic differentiation and fluid evolution processes.

The MAIC (ca 1525 Ma) is largely composed of K-rich, magnetite-bearing intrusive rocks that range in composition from quartz monzodiorite to biotite syenogranite and are cut by late, petrogenetically-related, alkali pegmatites and Na-rich balloon-textured albitites (Mark et al., 2004). This suite of intrusive rocks exhibit 'A-type' geochemical characteristics, and possess Y-undepleted, Sr-depleted compositions that implicate a derivation from partial melting of the mid-crust (<1.0-0.8 GPa; >850 ºC; Mark et al., 2004). Mantle derived dioritic intrusions were emplaced during the earliest phases of the complex's evolution, and are spatially associated with the localized occurrence of rocks of mingled and mixed derivation. A large, km-scale magmatic-hydrothermal breccia-vein system is hosted within the main phase of the MAIC, where the system grades from composite breccias filled with synchronously formed magmatic intrusions (e.g. pegmatites and albitites) and hydrothermal mineral precipitates in the topographic lows, to fracture-related hydrothermal vein systems in the topographic highs. Estimated temperatures from stable isotope mineral pair equilibrium (albite and quartz) for the evolved magmatic phases and hydrothermal

precipitates indicate formation temperatures ca. 550 ºC, which are consistent with temperature constraints from similar rocks elsewhere (cf. Mark and Foster, 2000; Perring et al., 2000; Mark et al., 2004). The MAIC exhibits many geochemical, mineralogical and textural similarities with Lightning Creek.

Granite Hosted Fluid Inclusions

Perring et al. (2000) documented hypersaline brine (type 1) and CO_2 (type 4) inclusions in high-temperature vein quartz and albite-quartz-magnetite sills at Lightning Creek (Table 3). Homogenization temperatures for type 1 inclusions are > 420 ºC with salinity ranging between 33 and 50 wt. % NaCl equiv. Type 4 CO_2 inclusions occur in primary zones spatially associated with type 1 inclusions and the CO_2 homogenizes via vapour bubble disappearance between 26.5 and 28.7 ºC. Type 2 and 3 inclusions commonly occur in the same trails in annealed microfractures (i.e. secondary) and have homogenization temperatures between 122 and 178 ºC. The inclusions are calcium-rich with estimated salinity comprising 8 to 25 wt % $CaCl_2$ and 3 to 7 wt. % NaCl. Also present within the Lightning Creek quartz veins are two phase aqueous inclusions with variable liquid-vapour ratios (Table 3). Only limited microthermometry has been carried out in the MAIC and Saxby granite systems (Fig. 10d and e). In terms of abundance type 1 multisolid inclusions are common and are typically postdated by type 2 and 3 inclusions. Mustard et al. (2005) documented complex type 1 inclusions that locally contained opaque phases including possible chalcopyrite (Fig. 10c). Type 4 CO_2 inclusions are rare in the MAIC but common in the Saxby granite and commonly occur with type 1 including mixed phases of brine and CO_2 in some inclusions (Mustard et al., 2005).

Granite	Setting	Type	Phases	Abundance	Th (C)	Salinity*	P (kbars)	References
Lightning Creek	Quartz veins & granite sills	1	L+V+nS	Abundant	>420	33 to 50	1.5 to 4	Perring et al., 2000
		2	L+V+/-S	Abundant	122 to 178	15 to 28		
		3	L+V, V+L	Common	178 to >370	<4.6		
		4	CO2	Common	26.5 to 28.7			
Mount Angelay	Syenite, pegmatite & aplite	1	L+V+nS	Abundant	>400	>50		Mark et al. 2004
		2	L+V+S	Common				
		3	L+V	Uncommon				
		4	CO2	Rare				
Saxby	Granite	1	L+V+nS	Common	No microthermometry data			Mustard et al., 2005
		2	L+V+S	Common				
		4	CO2	Abundant				

Table 3: Summary of fluid inclusion characteristics from granite-hosted magmatic-hydrothermal systems in the Cloncurry district. *NaCl wt % equiv.

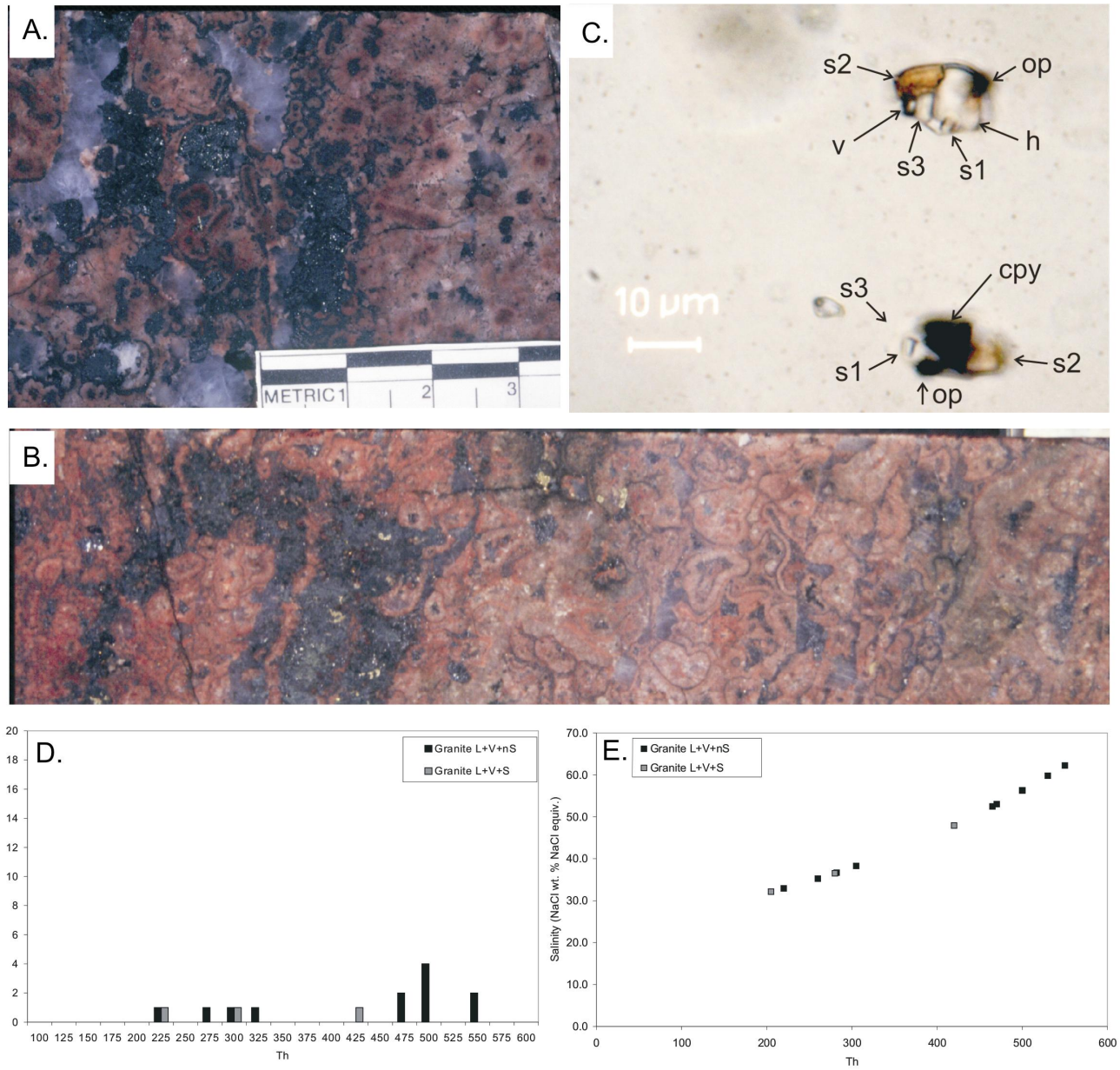

Figure 10: a. and b. Spherulitic texture in quartz-feldspar-magnetite-bearing sill representing part of the magmatic-hydrothermal transition at Lightning Creek (photograph courtesy of P.J. Pollard). c. Photomicrograph of type 1 multisolid fluid inclusions from MAIC containing likely chalcopyrite (triangular) crystal (possible trapped phase?; from Mustard et al., 2005). d. Histogram of homogenization temperatures (Th ºC) and e. Th versus salinity from Lightning Creek and Mount Angelay. The limited microthermometric data indicate the presence of both type 1 multisolid and type 2 halite-bearing fluid inclusions in the granite-hosted systems similar to that observed in the IOCG deposits.

2.4 Fluid Inclusion Chemistry

Fluid inclusion microanalysis has been carried out using PIXE, LAIPMS and laser Raman spectrometry within the F3 project (e.g., Baker, 2003; Mustard et al., 2004, 2005; Mark et al., 2004; Fu et al., 2004a and b). New IOCG PIXE data include analysis of fluid inclusions from Osborne and Starra (Table 4). The PIXE data presented here are from Osborne and Starra represent a subset of the total with the full dataset being evaluated as part of Louise Fisher's ongoing PhD research. In particular data excluded from this report include PIXE analyses that have suffered Cu interference during data collection (Mustard and Ryan, pers. com.). LAICPMS data from Osborne and Starra is also under evaluation as part of Fisher's PhD study. Additional PIXE data from Ernest Henry (Mark and Williams, unpub.) is included in this review as well as published data from Starra (Williams et al., 2001). Table 4 also presents new PIXE data collected from fluid inclusions from regional barren alteration systems (Fu et al., 2004a and b) and ongoing regional work includes LAICPMS analyses of fluid inclusions from barren breccia systems by Martina Bertelli in collaboration with Leeds University. Fluid inclusions from Eloise have also been analyzed as part of this collaboration and preliminary data is presented here. New PIXE data from fluid inclusions in granite hosted magmatic-hydrothermal systems includes data from the MAIC (Mark et al., 2004). Other data sets include Mustard et al. (2005) who presented LAICPMS data on the MAIC, Saxby granite and Lightning Creek system in addition to PIXE data from Lightning Creek (Perring et al., 2000).

IOCG Deposits

Type 1 inclusions from Osborne contain highly complex multisolid phases (Fig. 11a and b). Laser Raman analyses has identified the presence of solid phases including Fe-rich and Fe-poor ferropyrosmalite, calcite, magnetite and up to 3 separate salt phases. PIXE images show that salt phases present include sylvite and halite (Na shown via PIGE (gamma ray emission)). Calcium appears to occur mostly within the liquid phase of the inclusions. Copper displays a strong spatial association with magnetite (Fig. 11a) and iron-rich, Mn-poor ferropyrosmalite phase (Fig. 11b) and to a lesser degree with Fe- and Mn-rich ferropyrosmalite (both pyrosmalite phases were confirmed by laser Raman spectrometry; Fig. 11 a and b). The Cu signal may in part be due to a combination of $Si_{K\_}$ and $Fe_{K\_}$ signals from the host quartz and Fe-rich solid inclusion phases that create noise in the X-ray spectrum at the $Cu_{K\_}$ peak (Williams et al., 2004b). However, from the images it appears that Cu enrichment is selective (occurring in the Mn-poor ferropyrosmalite) despite both ferropyrosmalite phases being Fe-rich, and therefore not entirely a technique related phenomenom. Similar complex type 1 inclusions have been reported from Starra by Williams et al. (2001) and Mustard et al. (2004). In particular Ba-rich solid phases have been identified that in some cases are barite whereas in other instances may be chloride.

IOCG Locality	Osborne			Osborne			Osborne			Starra		
Fluid Inclusion Type	1			3			4			1		
No. Analyses	21			4			13			42		
Element	Average	Max	Min	Average	Max	Min	Average	Max	Min	Average	Max	Min
Cl	367387	479689	215502	117100	173000	63200	122145	310035	10538	298121	486000	157708
K	36520	83491	2544	6470	12200	3620	17020	47248	400	25671	87000	3800
Ca	11883	36007	1623	22970	50300	6480	6564	21900	1197	45399	92591	7269
Mn	6047	22258	753	482	1080	91	6766	15412	888	11105	27000	1950
Fe	66012	177853	13593	4335	7880	1140	49976	143865	10456	45458	162000	9660
Cu	142	254	63	120	228	52	145	429	40	1044	10434	123
Zn	895	2566	68	255	413	159	760	2151	95	2071	12449	319
As	102	706	32				270	854	44	1271	8009	68
Br	468	3364	73	212	247	130	767	2456	35	565	1595	87
Rb	422	1005	106	70	81	58	315	615	88	533	1304	121
Sr	503	1369	117	413	1210	52	289	790	76	1392	3300	462
Ba	2070	4818	267	1060	1060	1060	1234	2580	344	21954	80000	1790
Pb	824	2434	71	325	439	210	759	1924	243	915	2584	271
K/Ca	3.55	6.54	0.44	0.39	0.56	0.22	2.80	6.05	0.33	0.74	3.02	0.18
Mn/Fe	0.10	0.30	0.02	0.16	0.24	0.03	0.18	0.34	0.06	0.36	1.82	0.05
Br/Cl (x1000) mol ratios	0.45	1.00	0.16	0.90	1.40	0.62	4.97	25.41	0.13	0.93	1.82	0.22
IOCG Locality	Starra			Ernest Henry			Ernest Henry			Ernest Henry		
Fluid Inclusion Type	3			1			3			4		
No. Analyses	2			25			3			5		
Element	Average	Max	Min	Average	Max	Min	Average	Max	Min	Average	Max	Min
Cl	81150	92700	69600	277738	515300	142000	44100	63500	30700	1139	1595	810
K	974	1080	867	21058	175000	772	4410	4820	4000	819	2095	212
Ca	32500	40900	24100	16498	40610	1970	19200	22800	13100	1734	7000	102
Mn	86	115	56	33002	159000	288	49698	145899	606	920	2940	34
Fe	259	291	226	17807	191000	98	63919	190556	434	905	3017	48
Cu	38	42	33	160	767	30	144	256	76	68	102	32
Zn	53	63	42	2190	9100	99	941	2280	252	308	1080	33
As	31	50	12									
Br	112	134	89	260	1007	48	1139	2680	127	69	118	40
Rb	41	63	18	669	2818	106						
Sr	544	704	384	3445	16390	70	1420	1660	1180	460	800	119
Ba	663	698	628	13873	69550	860				1250	2540	525
Pb	71	94	48	1360	4750	149	1843	3204	481	237	363	120
K/Ca	0.03	0.04	0.03	1.30	5.26	0.08	0.27	0.37	0.18	1.62	2.65	0.11
Mn/Fe	0.32	0.40	0.25	5.78	18.28	0.07	2.51	5.97	0.77	0.95	1.71	0.19
Br/Cl (x1000) mol ratios	0.60	0.63	0.56	0.47	2.45	0.05	15.36	38.19	0.88	22.97	34.57	10.97
Locality	Barren regional alteration			Barren regional alteration			Barren regional alteration					
Fluid Inclusion Type	1			2			3					
No. Analyses	15			14			17					
Element	Average	Max	Min	Average	Max	Min	Average	Max	Min			
Cl	249293	314132	184991	222349	367419	175544	53190	234061	17618			
K	90012	217785	16911	43456	154321	5745	6048	40232	1010			
Ca	22070	50827	3430	29385	79113	2048	8972	21879	2284			
Mn	16281	51812	697	3369	8171	604	1276	15397	24			
Fe	68076	153313	4034	20803	61502	206	6726	68463	20			
Cu	277	659	50	211	437	40	131	292	23			
Zn	2147	4734	183	1254	5272	52	256	1426	22			
As	351	927	43	304	554	89	107	320	15			
Br	889	2001	190	780	2094	327	345	1093	47			
Rb	1542	4482	208	889	1684	198	379	1290	91			
Sr	1762	3746	187	1229	3027	163	692	1337	224			
Ba	6993	20375	807	3582	8190	1048	1866	7554	417			
Pb	1329	3843	262	681	1372	305	445	2452	35			
K/Ca	7.95	44.34	1.08	9.67	65.36	0.07	0.73	1.84	0.06			
Mn/Fe	0.24	0.65	0.05	0.54	2.93	0.07	0.77	2.85	0.01			
Br/Cl (x1000) mol ratios	1.63	4.10	0.35	1.64	5.22	0.54	4.06	14.75	0.62			
Granite Locality	MAIC			MAIC			MAIC			Lightning Creek		
Fluid Inclusion Type	1			2			3			1		
No. Analyses	15			4			4			5		
Element	Average	Max	Min	Average	Max	Min	Average	Max	Min	Average	Max	Min
Cl	296620	512716	153053	321388	394633	288288	221266	472349	90498	405000	440000	350000
K	20968	79567	5245	7366	11275	4130	5255	14757	2253	93800	163000	60000
Ca	29499	71612	3543	39302	51037	18331	26371	44700	7798	63200	98000	46000
Mn	5303	13750	49	1410	2499	483	1662	12108	22	4540	7000	3600
Fe	12096	41808	83	2145	4282	556	4679	53705	57	108000	130000	90000
Cu	388	3079	48	126	180	48	129	232	18	14200	19000	10000
Zn	601	1156	66	460	644	200	316	1073	45	630	933	499
As	516	1741	27	74	104	37	139	710	12			
Br	273	787	121	290	364	150	275	483	51	892	1500	564
Rb	1586	4186	96	278	372	187	449	2507	52	1116	1870	791
Sr	423	1066	79	481	652	354	359	790	66	913	1700	409
Ba	2030	4998	609	5459	7759	3650	3865	8358	1213	7686	10100	5740
Pb	989	4071	185	243	272	212	359	1426	49			
K/Ca	1.35	4.98	0.13	0.21	0.33	0.08	0.30	1.89	0.09	1.47	1.66	1.00
Mn/Fe	1.05	6.30	0.26	0.68	0.87	0.48	0.60	2.96	0.00	0.04	0.07	0.03
Br/Cl (x1000) mol ratios	0.45	1.24	0.11	0.41	0.52	0.17	0.65	1.84	0.10	1.02	1.60	0.59

Table 4: Summary of IOCG PIXE data (see text for data source).

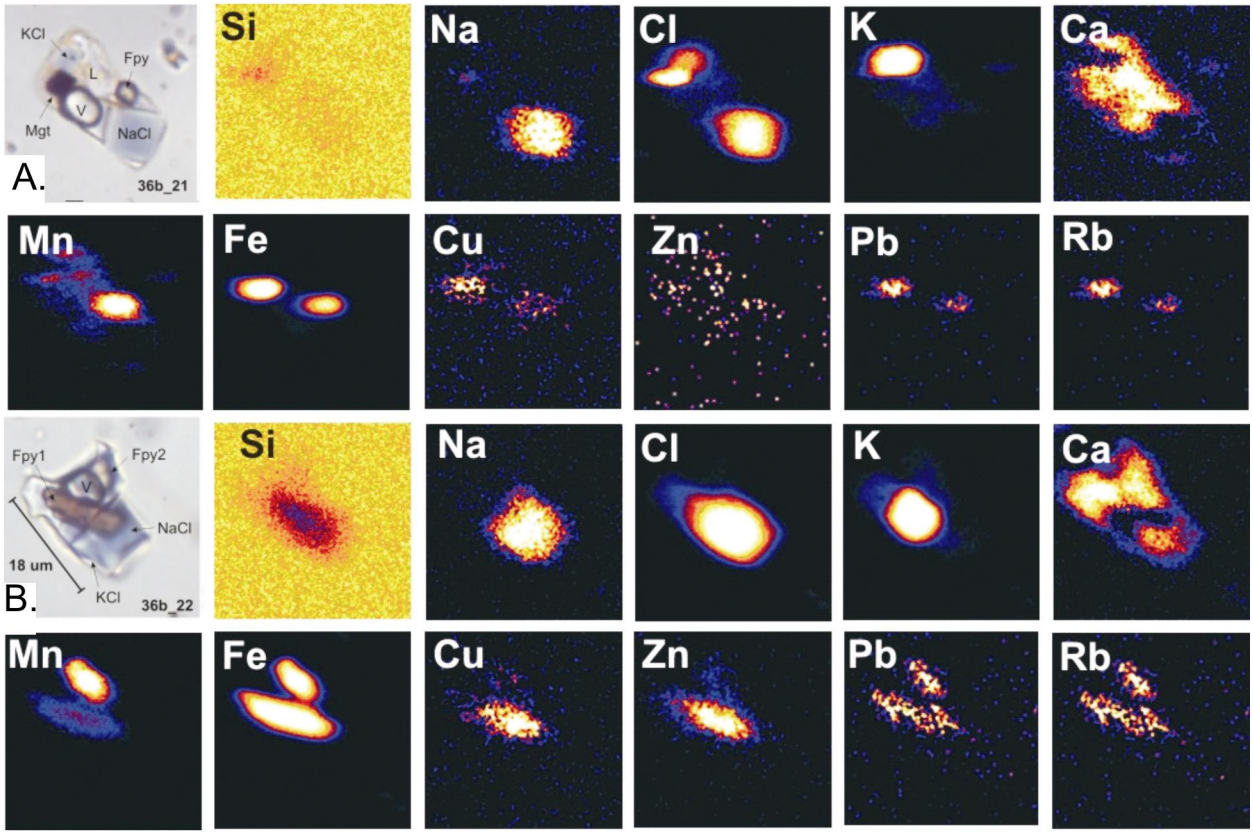

Figure 11. (a) and (b) type 1 multi-solid fluid inclusions associated with pre to syn-mineralisation stages at Osborne Cu-Au deposit. Fpy = ferropyrosmalite, NaCl = Halite, KCl = Sylvite, Cal = Calcite, Mgt = Magnetite.

PIXE analyses of Type 1 inclusions from Osborne have chlorine contents of between ~215,000 and 500,000 ppm (~35 to 80 wt. % NaCl equiv.) which are consistent with microthermometric studies (Tables 1 and 4). The inclusions contain high concentrations of Fe (~ 13,500 to 180,000ppm), K (~2,500 to 85,000ppm) and Ca (~1,500 to 36,000 ppm) and have high K/Ca ratios (average 3.55). Type 1 inclusions from Starra are similar with high Cl (~160,000 to 486,000ppm), Fe (~10,000 to 162,000ppm), and K (~3,800 to 87,000ppm) but with notably higher Ca (~7,000 to 92,500ppm). Starra inclusions therefore have lower K/Ca ratios (average ~0.74). Preliminary LAICPMS analysis of type 1 and 2 inclusions from Eloise indicate that type 1 inclusions have K/Ca ratios mostly >0.3 and type 2 inclusions have K/Ca <0.3. Base metal contents at Osborne are on the order of 60 to 250 ppm for Cu, 70 to 2,500 ppm for Zn and Pb whereas Starra type 1 inclusions contain much higher concentrations of base metals with averages of ~1,000 ppm (Table 4). Starra type 1 inclusions contain very high concentrations of Ba which are on average an order of magnitude greater than Osborne (~22,000 versus 2,000 ppm). Br/Cl (x1000) mol ratios range from <0.16 to 1.00 at Osborne and 0.22 to 1.82 at Starra in type 1 inclusions.

PIXE analyses of end-member type 4 inclusions from Ernest Henry illustrate their low salinity and low solute contents compared to more saline inclusion types (Table 4). Type 4 inclusions analyzed from Osborne represent mixed brine-CO_2 types (Fig. 7). PIXE and normal photomicrograph images of the mixed inclusions reveal variable solid phases present including halite, sylvite, ferropyrosmalite and calcite.

The liquid CO_2 inclusions contained minor N_2 and CH_4. Since the fluid inclusions have trapped heterogeneous fluids their chemistry will represent mixtures and are not representative of an end-member fluid phase. Ongoing research by Louise Fisher is currently evaluating the significance of these data. Type 3 inclusions from Starra and Ernest Henry have low K/Ca ratios (0.03 to 0.04) and low transition and base metal contents compared to type 1 inclusions (Table 4).

Barren Regional Alteration Systems

Type 1 inclusions are rare to absent in many of the barren regional alteration systems, however, Fu et al. (2004a and b) have described them from sodic-calcic alteration around Cloncurry and locally in the Mary Kathleen Fold Belt (Fig. 12a). PIXE, laser Raman and petrographic studies reveal that type 1 inclusions in these settings contain a large halite cube together with one to five other solid phases such as sylvite, calcite, hematite and/or magnetite, and a vapour bubble (~ 5 vol. %) at room temperature. No sulfide or sulfate daughter phases have been identified. The chemistry of type 1 inclusions is similar to those analyzed in IOCG deposits with high Cl, K, Ca and Fe contents and similar ranges for base metals, however, Br/Cl (x1000) mol ratios are distinctly higher on average (Table 4).

Type 2 inclusions have on average lower K, Ca, Fe and base metal contents than type 1 inclusions and K/Ca ratios are highly variable (Table 4 and Fig. 12b). Average Br/Cl ratios are similar to regional type 1 inclusions. Type 3 inclusions have the low K/Ca ratios (average 0.73) and high Br/Cl ratios (average 4.06) compared to regional type 1 and 2 inclusions. Type 3 inclusions also have on average lower Fe and base metal contents (Table 4 and Fig. 12c).

Barren Granite Hosted Magmatic-Hydrothermal Systems

Mark et al. (2004) presented 33 PIXE analyses from the MAIC (Table 4). Type 1, 2 and 3 inclusions exhibit similar variations to those observed in regional and IOCG settings in that the high salinity type 1 inclusions contain highest concentrations of K, Ca and Fe and the K/Ca ratios are lower in type 2 and 3 inclusions. Base metal contents are on average highest in type 1 inclusions with Cu locally reaching 3,000 ppm. Barium, however, has a higher concentration in type 2 and 3 inclusions than type 1 inclusions. Br/Cl (x1000) mol ratios average around 0.5 for all inclusion types (Table 4). K/Ca ratios of type 1 inclusions at Lightning Creek are similar to type 1 inclusions in the MAIC but the Lightning Creek inclusions are noted for their particularly high Fe (90,000 to 130,000 ppm) and Cu (10,000 to 19,000 ppm) contents (Perring et al., 2000). Type 1 inclusions from Lightning Creek have Br/Cl (x1000) mol ratios of 0.59 to 1.6.

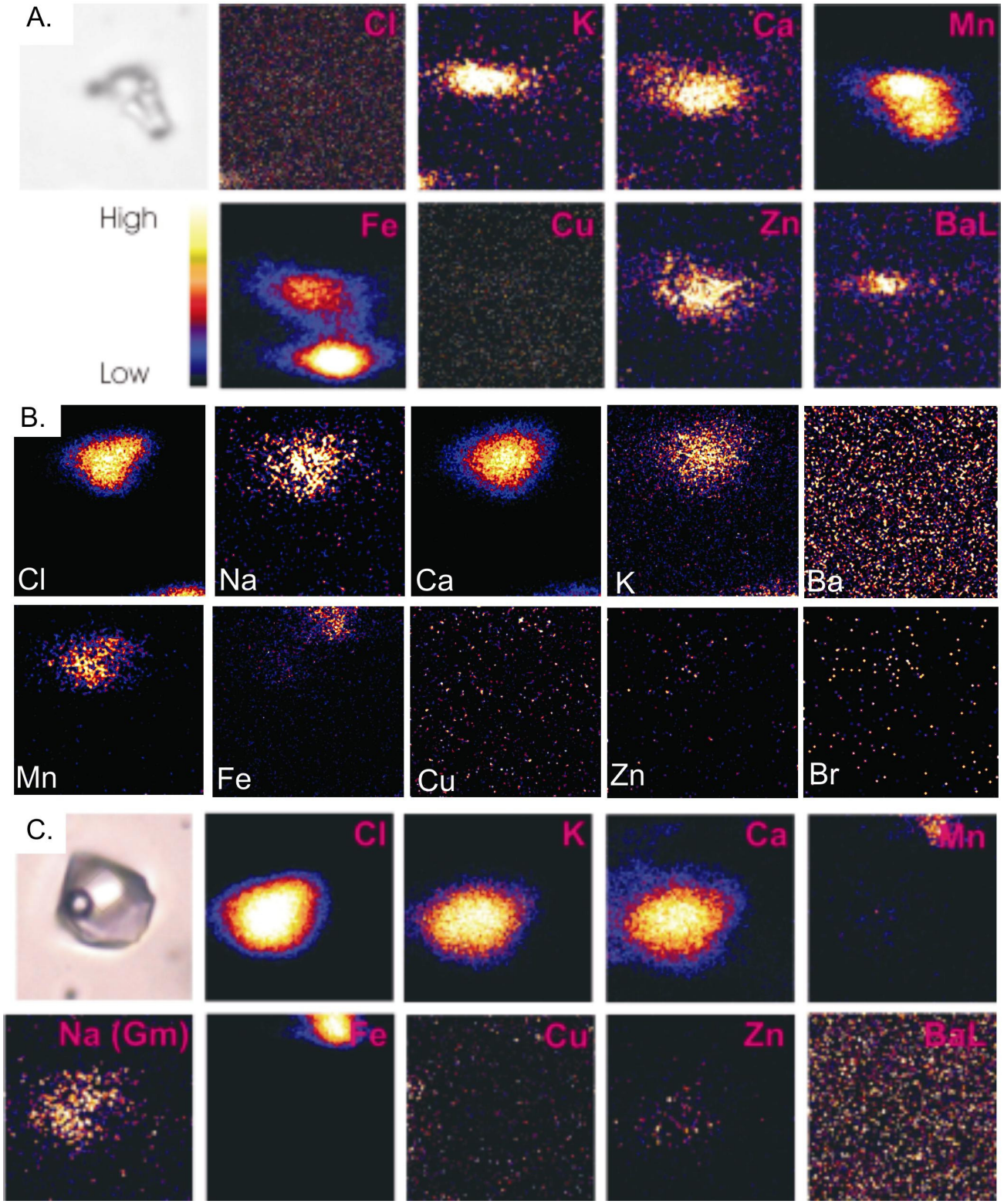

Figure 12. PIXE images of fluid inclusions in regional barren alteration. a. Type 1 multisolid inclusion from Mary Kathleen (inclusion size 10 by 6 µm; inclusion 02CC31_1). b. Type 2 halite-bearing inclusion from Mount Averice (box scale 20x20 µm; inclusion CC147_A4). c. Type 3 two phase aqueous inclusion from Knobby (inclusion size 9 by 8 µm; inclusion 02CC94B).

Mustard et al. (2005) reported LAICPMS analysis of 29 fluid inclusions from Mount Angelay and Lightning Creek (Table 5). The fluid inclusions from Mount Angelay represented primary multi-solid inclusions (type 1) hosted in quartz from aplite and pegmatite, whereas those from Lightning Creek comprise 11 primary multi-solid inclusions (type 1) and 2 pseudo-secondary to secondary CO_2-bearing (type 4) inclusions hosted in quartz from a spherulitic, iron-rich, quartz feldspar sill. The LAICPMS results from the MAIC type 1 inclusions suggest higher Ca contents than K and that Cu contents average ~4000 ppm. Lightning Creek type 1 inclusions are consistent with PIXE data presented by Perring et al (2000) with higher K than Ca, and Cu contents ranging from 2,600 to 8,000 ppm.

Location	Mount Angelay			Mount Angelay			Lightning Creek			Lightning Creek			Lightning Creek		
Salinity	60 wt% equiv			60 wt% equiv			40.5 wt% equiv			40.5 wt% equiv			5 wt% equiv		
Description	multi-solid brine with opaque			lvh+1 solid			multi-solid brine with opaque			brine, with hematite			CO_2		
Analyses	n=9			n=7			n=8			n=3			n=2		
Element	Average	Max	Min	Average	Max	Min	Average	Max	Min	Average	Max	Min	Average	Max	Min
B11	2952	6294	451	536	1402	102	451	807	131	634	1307	268	349	349	349
Na23	160442	225090	32618	141343	192540	6234	92508	114683	45056	103098	128953	88826	19700	19700	19700
Mg24	111	202	14	325	923	30	60	126	12	29	52	17	BDL	BDL	BDL
K39	63488	172741	19755	59831	121520	25180	53548	108572	16339	32309	41350	21328	6503	12145	861
Ca43	104509	302065	12639	102560	383235	16413	33713	109905	8629	47198	65112	21916	2132	2132	2132
Ti47	4983	18803	19	372	1058	108	1511	3850	133	BDL	BDL	BDL	172	172	172
V51	BDL	BDL	BDL	11	29	1	BDL	BDL	BDL	BDL	BDL	BDL	BDL	BDL	BDL
Cr52	2083	4390	68	239	588	56	269	712	78	246	493	86	44	44	44
Mn55	4225	7257	1405	6071	24567	379	2060	5833	683	6471	10815	2853	156	156	156
Fe57	50011	79557	1036	28295	46089	1006	38910	47428	16532	33874	44576	19902	1438	1438	1438
Ni58	1242	3326	228	337	728	165	204	238	89	216	335	155	BDL	BDL	BDL
Co59	11	17	6	4	7	1	9	21	4	27	56	11	BDL	BDL	BDL
Zn64	1083	4352	174	709	2192	212	164	588	46	685	995	496	99	99	99
Cu65	4033	8071	20	396	1684	11	6280	9020	2636	72	179	13	20	20	20
Zn66	983	4354	184	683	2381	199	167	623	47	758	1164	531	80	80	80
As75	457	1073	34	108	268	22	16	36	8	52	75	28	BDL	BDL	BDL
Rb85	8178	51653	463	1476	3082	612	386	1120	141	785	1131	431	9	9	9
Sr88	1687	4568	72	1763	4976	436	308	1033	27	1126	1462	661	14	26	3
Mo98	31	51	11	5	7	2	13	24	5	BDL	BDL	BDL	BDL	BDL	BDL
Ag109	BDL	BDL	BDL	2.2	4	1	0.4	0.4	BDL	0.4	BDL	BDL	BDL	BDL	BDL
Cs133	1394	4619	106	173	439	26	24	53	7	89	104	59	5	7	3
Ba137	2093	6356	142	3018	5591	659	844	1865	167	2905	4715	1473	19	19	19
Au197	BDL	BDL	BDL	BDL	2	BDL	BDL	BDL	BDL	BDL	BDL	BDL	BDL	BDL	BDL
Pb208	317	644	20	162	473	57	32	118	7	38	43	30	7	7	7
Bi209	40	78	10	4	12	2	1	1	BDL	2	3	BDL	2	2	2
U238	13	21	5	18	31	4	5	8	BDL	BDL	BDL	BDL	BDL	BDL	BDL

All concentrations in ppm

Table 5: LAICPMS analysis of fluid inclusions from MAIC and Lightning Creek (from Mustard et al., 2005)

2.5 Comparison of the Fluid Inclusion Chemistry of IOCG Deposits, Barren Regional and Granite Hosted Hydrothermal Systems

A key difference between fluid inclusions within barren regional alteration and the IOCG deposits and granite-hosted magmatic-hydrothermal systems is the abundance of type 1 multisolid inclusions in the latter two environments. Type 1 inclusions are rare to absent in the barren regional alteration systems with type 2 and 3 inclusions most abundant. Type 1 inclusions are characterized by higher homogenization temperatures and salinity than types 2 and 3 and consequently they contain greater concentrations of solutes (Table 4). Type 1 inclusions typically have higher K/Ca ratios than type 2 and 3 inclusions although this does vary depending on setting (Fig. 13). For example, Starra type 1 inclusions have on average lower K than Ca whereas Osborne type 1 inclusions have average K/Ca ratios of ~3.5 (Table 4). In the barren regional alteration settings K/Ca ratios for type 1 inclusions are >1, however, type 2 inclusions are highly variable with two main population, one with K/Ca > 2 and the other <1 (Fig. 13). Granite hosted fluid inclusions at Lightning Creek have consistently higher K than Ca whereas type 1 inclusions from the MAIC have variable K/Ca ratios. Type 2 and 3 inclusions in the MAIC have K/Ca ratios

<1. High K/Ca ratios are commonly characteristic of high temperature fluids particularly in magmatic environments whereas lower temperature crustal brines or magmatic fluids that have cooled and equilibrated with granites and/or country rocks are commonly characterized by low K/Ca ratios (cf. Whitney et al., 1985).

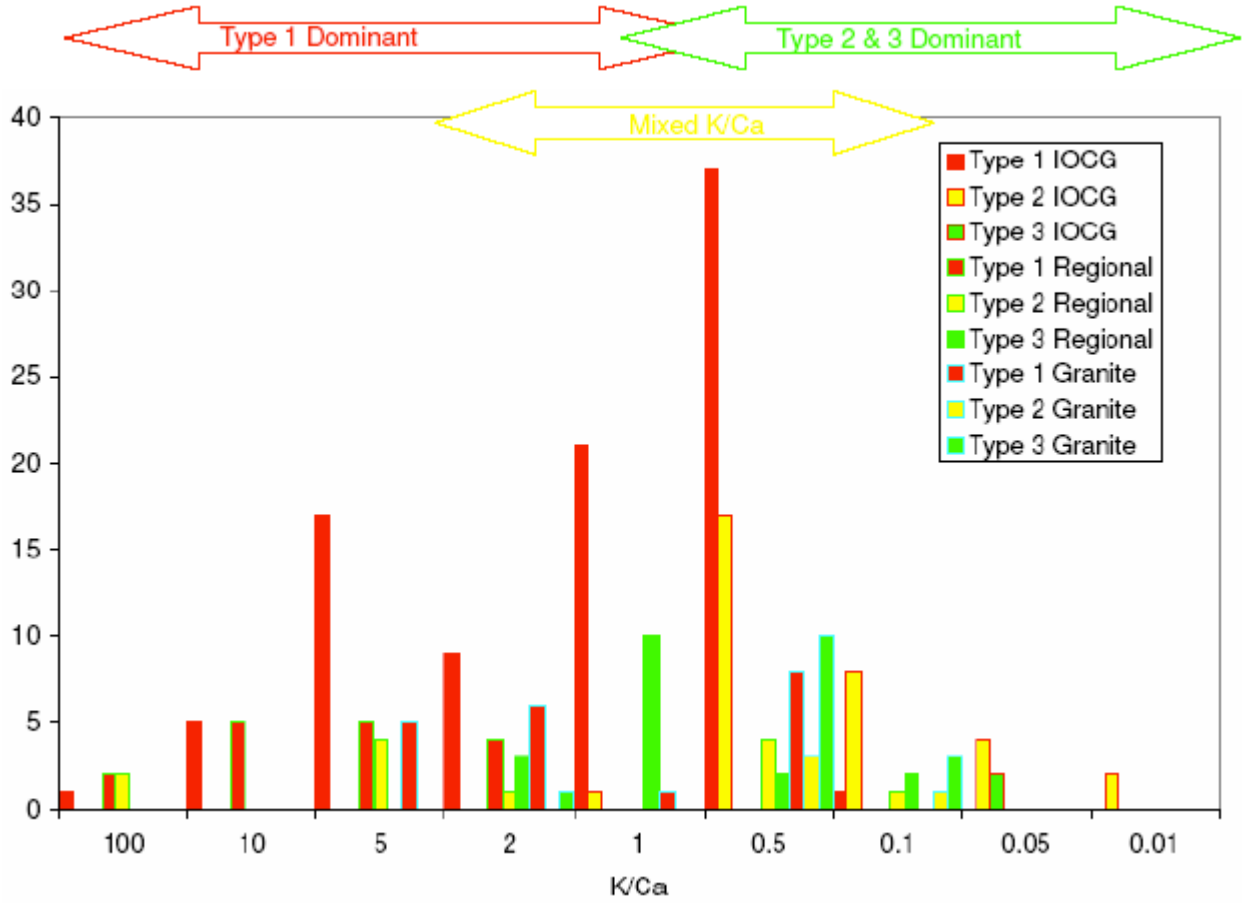

Figure 13. K/Ca ratios for type 1 multisolid, type 2 halite-bearing and type 3 two phase aqueous inclusions in IOCG, regional and granite hosted environments. Typically type 1 inclusions have higher K/Ca ratios than type 2 and 3 inclusions, however, there is significant overlap that may reflect fluid mixing and/or equilibration with different host rocks.

The presence of type 1 inclusions in IOCG systems and their low abundance in barren regional alteration settings suggest that these fluids were critical ingredients in the formation of the deposits. Copper is likely to be transported as a chloride complex in such environments, therefore, the more chlorine available the greater the metal carrying capacity of the fluid. This is supported by the PIXE analyses that show type 1 inclusions typically contain the highest Cu contents whether in IOCG deposits or barren regional or granite hosted environments (Fig. 14). However, in detail the interpretation is more complex. Type 1 inclusions from Starra contain some of the highest Cu contents of any IOCG deposits studied (average ~ 1000ppm; cf. Williams et al., 2001) whereas Osborne and Ernest Henry type 1 inclusions have Cu values less than type 1 inclusions in barren regional settings (average ~ 150 ppm versus 275 ppm; Table 4). This may be related to issues of carrier versus spent fluid and/or entrapment during Cu deposition. The high Cu contents in type 1 inclusions at Starra have been interpreted to represent Cu-rich parent or carrier

fluids (Williams et al. 2001). Similarly the high Cu contents of type 1 inclusions at Lightning Creek, and locally in the MAIC (Mustard et al. 2005) suggest that high salinity, high temperature fluids in magmatic environments were capable of transporting significant quantities of Cu (Perring et al., 2000; Mustard et al., 2005).

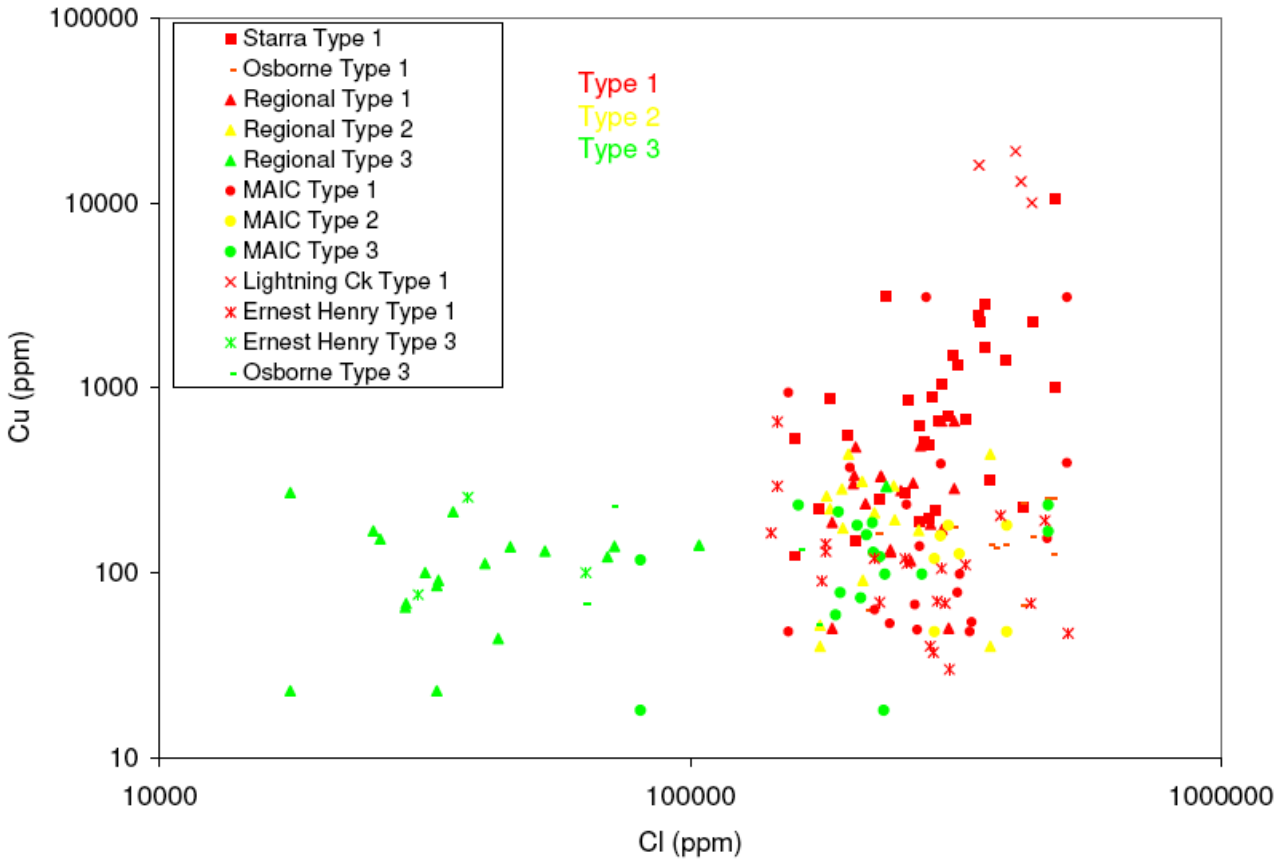

Figure 14. Cu versus Cl scatter plot for type 1 multisolid, type 2 halite-bearing and type 3 two phase aqueous inclusions in IOCG, regional and granite hosted environments. Typically type 1 inclusions have higher Cu contents than type 2 and 3 inclusions.

The key to Cu deposition and hence deposit formation is the availability of S which unfortunately has an atomic mass too low to be quantitatively measured using PIXE. Perring et al. (2000) suggested that the Cu-rich fluids at Lightning Creek did not precipitate Cu because of low S activity and high temperature magmatic nature of the prospect. Mustard et al. (2005) recognized sulfide daughter phases in type 1 brines in the MAIC suggesting some S was present in certain igneous environments in the Cloncurry district (Fig. 10c). Williams et al. (2001) has highlighted the fact that high Ba contents of fluid inclusions in IOCG deposits is also indicative of S-poor fluids due to the low solubility of Ba in S-bearing fluids. There is a weak positive correlation between Cu and Ba in all fluid inclusions from the Cloncurry district suggesting that Ba-rich, and potentially sulfate-poor, fluids were responsible for transporting Cu (Fig. 15).

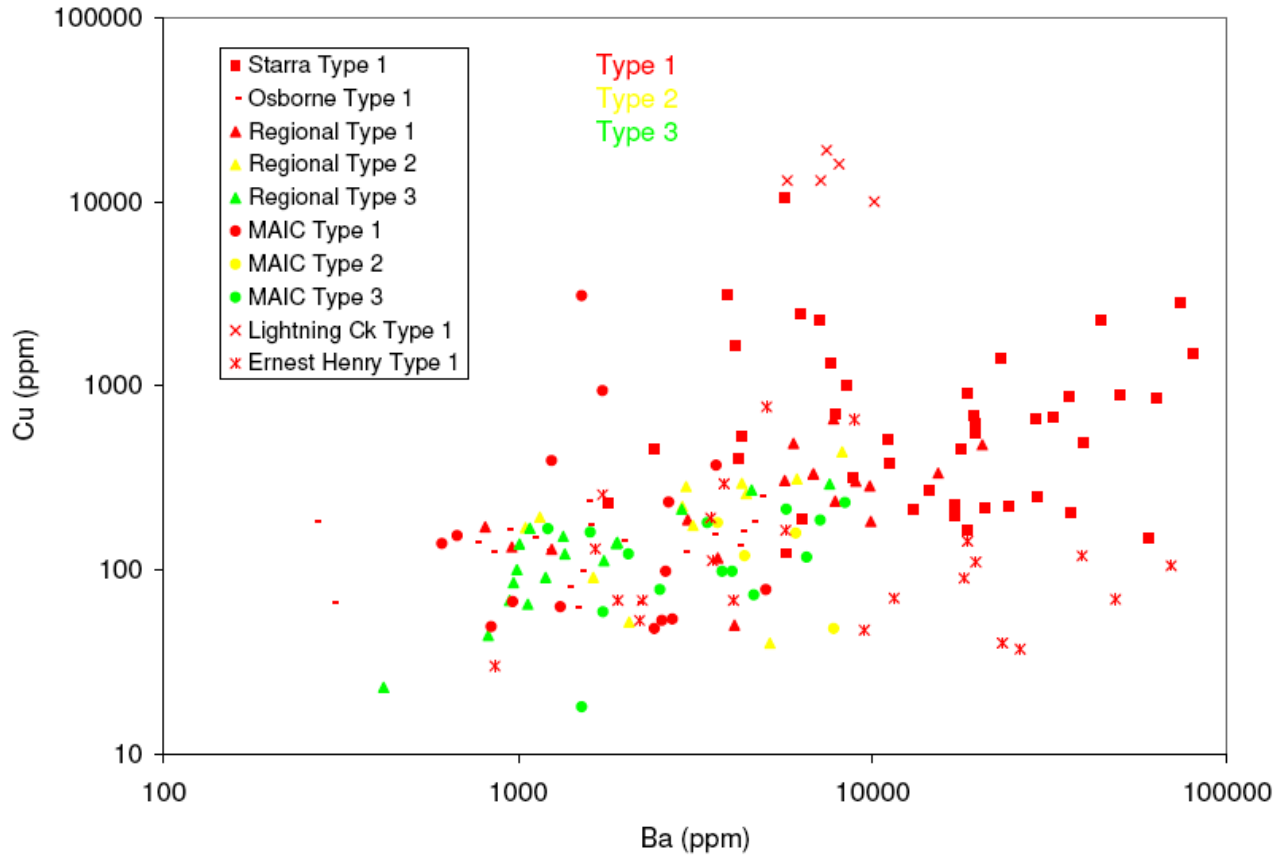

Figure 15. Cu versus Ba scatter plot for type 1 multisolid, type 2 halite-bearing and type 3 two phase aqueous inclusions in IOCG, regional and granite hosted environments. Note the weak, positive correlation between Cu and Ba consistent with Cu-rich, S-poor (high Ba) carrier fluids.

Fluid sources have been widely debated in IOCG deposit genesis with arguments focussed upon the relative contributions of magmatic and/or evporite-related fluid salinity (e.g., Hitzman et al., 1992; Barton and Johnson, 1996; Pollard, 2000). Bromine and chlorine are widely used as tracers for salinity source (e.g., Bohlke and Irwin, 1992) due to fractionation processes unique to certain environments such as seawater evaporation (resulting in increased Br/Cl ratios in the brine derived from the seawater) and halite precipitation and re-dissolution (resulting in decreased Br/Cl ratios due to the preferential take up of chlorine over bromine in halite). Bohlke and Irwin (1992) also compiled Br/Cl ratios from volcanic fumaroles in order to characterize magmatic fluids and suggested that the bulk of the data lie below the Br/Cl mol ratio of seawater ($1.54x10^{-3}$) mostly between $0.5x10^{-3}$ and $1.0x10^{-3}$ with outliers of the data ranging between $0.2x10^{-3}$ to $2.0\ x10^{-3}$. Williams et al. (2001) and Perring et al. (2000) have reported Br and Cl data from PIXE analysis of fluid inclusions that show Lightning Creek type 1 inclusions have Br/Cl ratios consistent with a magmatic source whereas Starra and Osborne have ratios that may reflect magmatic and halite-dissolution derived salinity. New data collected in F3 from IOCG deposits, barren regional alteration systems and granite-hosted environment have distinct Br/Cl ratios (Fig. 16). The Br/Cl mol ratios from type 1, 2 and 3 inclusions (type 4 inclusions from Osborne have been omitted due to the heterogeneous nature of the fluid inclusions) in IOCG deposits and granite hosted environments have similar ranges with all data falling below $1.84x10^{-3}$ to values of $<0.16x10^{-3}$. This could be interpreted as a mixture of magmatic and halite-dissolution derived salinity in both environments and suggests that neither

types 1, 2 nor 3 inclusions contain halogens from a unique magmatic or dissolved halite source. Type 1, 2 and 3 inclusions from barren regional alteration systems have Br/Cl ratios above $0.35x10^{-3}$ with a significant proportion above seawater and in the bittern brine field (> $1.54x10^{-3}$). The data therefore imply that barren regional alteration systems derived their salinity mostly from a different source than the IOCG and granite-hosted environments.

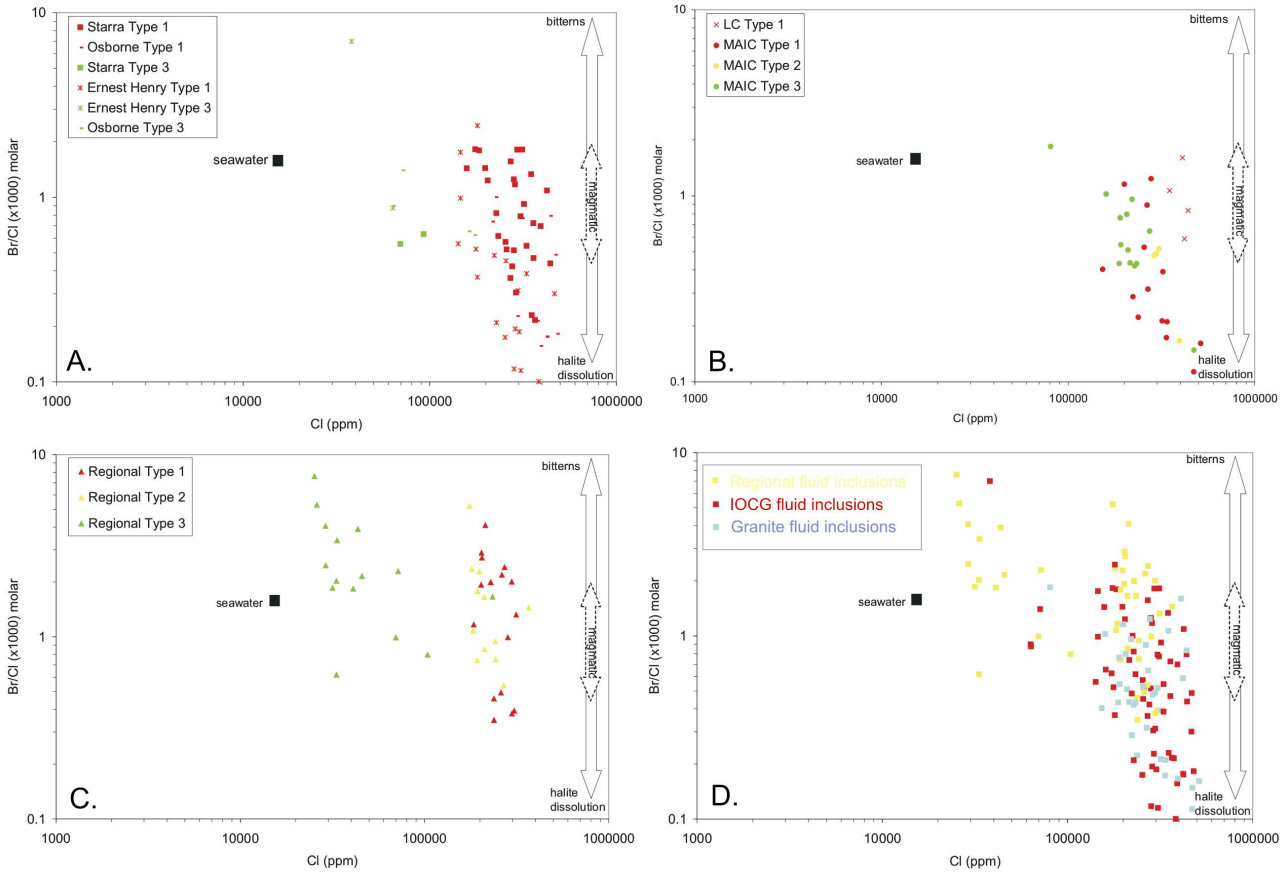

Figure 16. Br/Cl (x1000) mol ratios versus Cl (ppm) for fluid inclusions in (a) IOCG, (b) granite and (c) regional alteration settings. d. Illustrates that fluid inclusions in regional barren alteration setting typically have higher Br/Cl ratios than IOCG and granite-hosted environments.

The highest Cu contents of fluid inclusions have been recorded from Lightning Creek and Br/Cl ratios in this setting are consistent with a magmatic source (Perring et al., 2000). Analyses of Cu and Br/Cl from all the data compiled here suggest that the highest Cu contents are in inclusions with Br/Cl consistent with a magmatic origin and the spread of data may be interpreted as representing mixing between three fluid end-members i.e. high Cu-bearing magmatic fluids and low Cu-bearing halite dissolution and bittern derived fluids (Fig. 17).

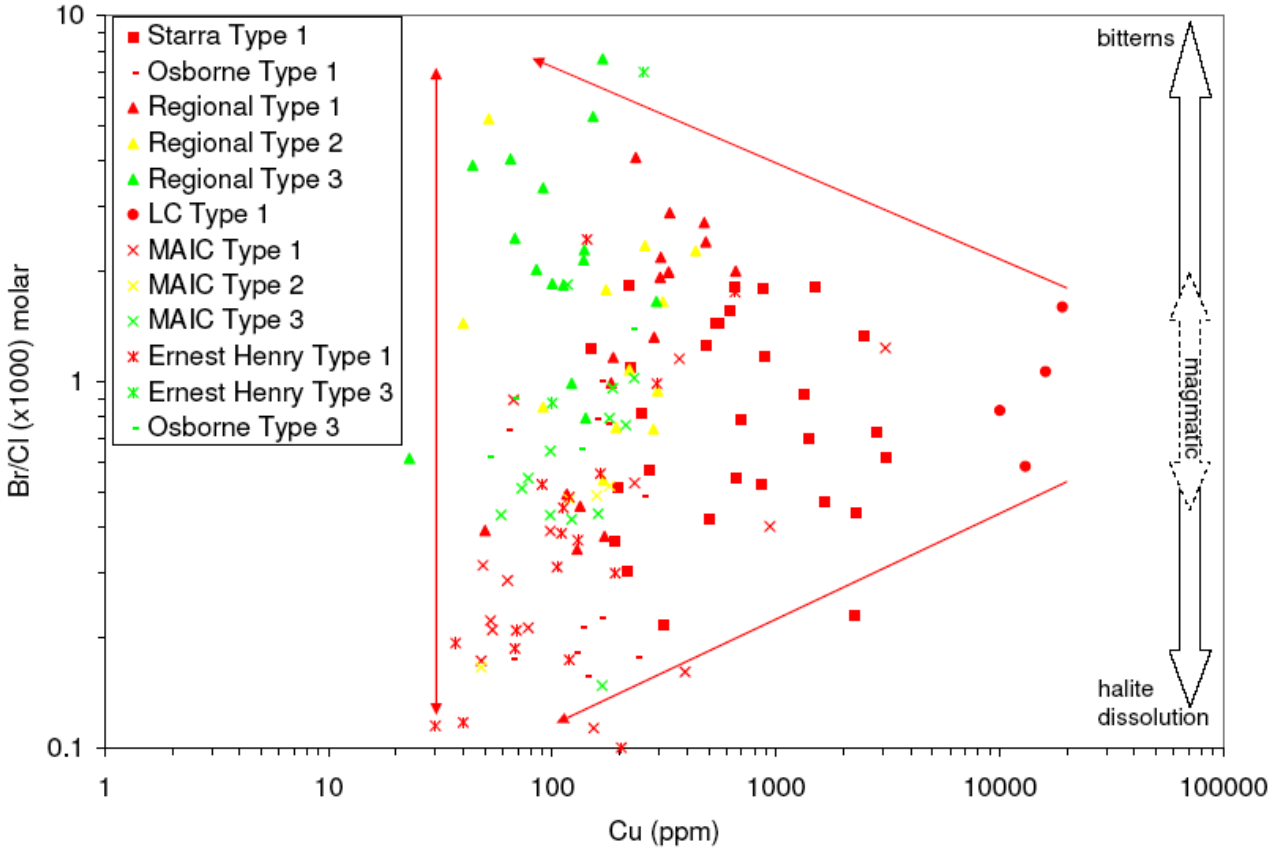

Figure 17. Br/Cl (x1000) mol ratios versus Cu (ppm) for fluid inclusions in (a) IOCG, (b) granite and (c) regional alteration settings. The data suggests that the highest Cu contents are found in fluid inclusions with Br/Cl ratios consistent with magmatic fluids and that the overall distribution of data could be interpreted in terms of mixing between high Cu-bearing magmatic fluids and low Cu-bearing halite dissolution and bittern derived fluids.

2.6 Comparison with Noble Gas and Halogen Data from Step Heating Analysis

The PIXE results described above are consistent with step heating noble gas and halogen analysis carried out in collaboration with the H4 project. Twenty nine quartz samples selected from IOCG deposits and regional veins in the Eastern Succession have been analysed by detailed stepped heating experiments. Gas extracted by stepped heating between 200 and 700 ºC can be related to the decrepitation temperatures of different fluid inclusion types that are observed during microthermometry. Stepped heating therefore reveals the total variation of fluid compositions trapped by a single sample (Fig. 18). To date six regional veins and a twenty three IOCG samples from Ernest Henry, Osborne, Starra and Eloise have been analysed. The data exhibit considerable variability reflecting the presence of several fluid types within the district at the time of mineralization.

In general the IOCG samples exhibit a spread in Br/Cl and I/Cl values between 0.3-2x10^{-3} and 1.5-20x10^{-6}, respectively. The maximum values overlap those of Porphyry Copper Deposit fluids that are considered to have had a juvenile magmatic origin (Kendrick et al., 2001) and the composition of fluids in mantle

diamond (Johnson et al., 2000). The minimum values are slightly above those measured in crustal fluids that have dissolved halite, such as in the Hansonburg MVT (Bohlke and Irwin, 1992). The majority of regional samples analysed have elevated Br/Cl values of $>2x10^{-3}$ indicating involvement of bittern brines (Zherebstova and Volkova, 1966), but two of the samples have low Br/Cl values indicative of halite dissolution (Fig. 20). Therefore, the regional quartz veins provide evidence for the evaporation of seawater beyond the point of halite saturation. Partial dissolution of the evaporites (incongruent dissolution) explains the minimum Br/Cl and I/Cl compositions that are slightly above those of halite.

The $^{40}Ar/^{36}Ar$ values of most IOCG deposits are less than ~2000. These low values are an order of magnitude lower than the MORB mantle value of >40,000 (Burnard et al., 1999) and suggest a component of surface derived meteoric water is present in all the deposits. Similarly, the regional fluids have maximum $^{40}Ar/^{36}Ar$ values of slightly above 2000, but are predominantly in the range 500-1000, compatible with surface derived fluids that have acquired $^{40}Ar_E$ by interaction with diverse crustal rocks over varying periods of crustal residence.

The maximum $^{40}Ar/^{36}Ar$ value of ~29,000 was measured for the Ernest Henry sample with the most mantle like halogen signature (Fig. 18). The correlation between mantle-like Ar and halogen signatures is most easily explained by mixing between a juvenile magmatic fluid derived from A-type granites, with an ultimate mantle origin, and halite dissolution waters (Fig. 18). To date, the range of compositions determined for most of the Osborne, Starra and Eloise samples are compatible with a similar origin; differences in the $^{40}Ar/^{36}Ar$ compositions may be explained by differential devolatilisation histories in the different deposits. However, two Osborne samples have Br/Cl above the range of mantle values and the mixing trend could alternatively be explained by mixing between crustal fluids (bittern brines) seen in the regional samples and halite dissolution waters that predominate in the deposits.

There is little evidence for a magmatic component in any of the regional fluid samples. Although a juvenile magmatic fluid could have been present at each of the deposits, the evidence is only strong for Ernest Henry that has the highest $^{40}Ar/^{36}Ar$ values. Of the samples studied to date the highest salinity multi solid fluid inclusions with salinities of up to 65 wt % are characterized by the lowest Br/Cl and I/Cl values (gas released between 500-700 ºC by stepped heating), perhaps suggesting that halite dissolution appears to be a more important source of salinity than magma crystallization. Finally, feldspar extracted from a pegmatite at Osborne (sample OS852) includes fluids with a mantle like halogen signature and $^{40}Ar/^{36}Ar$ similar to the quartz samples; <2000. However, the $^{40}Ar/^{36}Ar$ value of lattice hosted Ar is similar to the maximum values for Ernest Henry ~20,000. This sample may indicate that either mantle heat was involved in crustal melting at Osborne, or that the mantle like fluid end-member involved in mineralization at all of the deposits is actually a crustal melt.

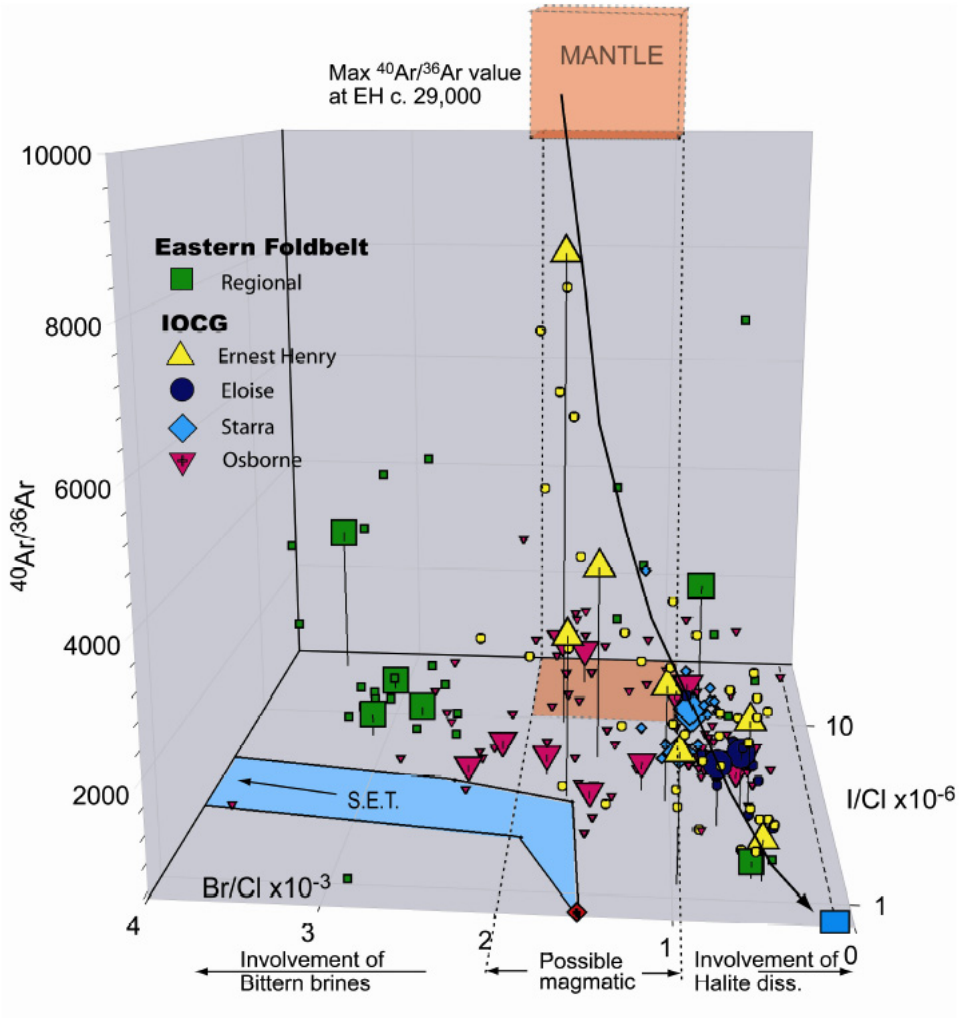

Figure 18: 3D multi-component composition plot for IOCG deposits and regional veins of the Eastern Succession of the Mt Isa Inlier. In order to maximize spatial separation of data points BrCl and $^{40}Ar/^{36}Ar$ are plotted linearly while I/Cl is plotted on a logarithmic scale. The highest $^{40}Ar/^{36}Ar$ data points from Ernest Henry and the field of MORB mantle compositions ($^{40}Ar/^{36}Ar$ >40,000) plot above the graph area. Large symbols indicate the average compositions determined by stepped heating between 200 to 700 ºC. The small symbols indicate the composition of individual steps and show the total intra-sample variability. See Kendrick et al. (2005; available on Twiki) for source data and references.

3.0 Comparison with IOCG breccias in the Wernecke Mountains, Canada

The Wernecke Mountains, Canada, represent a poorly explored and studied Proterozoic terrane that contains numerous IOCG occurrences but no significant deposits. The Wernecke Mountains were selected in order to compare and contrast processes of forming IOCG systems in sedimentary basins that have undergone lower grade metamorphism and deformation and which lack felsic magmatism compared with the Cloncurry district. The research presented here forms part of a PhD completed in 2004 by Julie Hunt (sponsored by the Yukon Geological Survey; see Appendix) with additional contributions from David Gillen who is currently carrying out detailed fluid chemistry research on fluid inclusions from the Wernecke Mountains as part of ongoing F3 research.

3.1 Geological Setting and IOCG Breccias

In the Yukon, Canada, IOCG mineralization and extensive metasomatic alteration are associated with an ?Early to mid-Proterozoic breccia system known as Wernecke Breccia that extends east-west for several hundred kilometres in the north central part of the terittory (Fig. 19; *cf.* Bell, 1986; Thorkelson, 2000). Wernecke Breccia occurs in areas underlain by the Wernecke Supergroup (WSG) a ~ 13 km-thick package of Early Proterozoic dominantly marine, fine-grained sedimentary rocks and carbonates that were deposited as two clastic to carbonate grand cycles (Fig. 20; Delaney, 1981; Thorkelson, 2000). Small Early Proterozoic (*ca*. 1710 Ma) mafic to intermediate igneous bodies, known as Bonnet Plume River Intrusions (BPRI), crosscut the WSG and occur as clasts in Wernecke Breccia (Thorkelson, 2000; Thorkelson *et al.,* 2001a,b). Rare mafic to intermediate subaerial volcanic rocks, known as the Slab volcanics, also occur in this area but have only been observed as clasts in Wernecke Breccia bodies in the lower part of the WSG at the eastern-end of the breccia system (*cf.* Thorkelson, 2000; Laughton, 2004).

Strata of the WSG were deformed and metamorphosed to greenschist grade during the Racklan orogeny, a period of contractional deformation that occurred prior to 1600 Ma (*cf.* Thorkelson, 2000; Thorkelson *et al.*, 2001b; Brideau *et al.*, 2002). The distribution of strain throughout the WSG was heterogeneous and resulted in schist belts flanked by relatively undeformed rocks many of which retain original sedimentary structures (*ibid*.). The timing of BPRI and Slab volcanics relative to Racklan deformation is uncertain (Thorkelson, 2000; Thorkelson *et al.*, 2001b; Laughton, 2004).

Bodies of clast- to matrix-supported Wernecke Breccia range from a few centimetres to several kilometres across and can be discordant or parallel to layering in WSG with no or numerous offshoots and contacts that vary from sharp to gradational (*cf.* Delaney, 1981; Bell, 1986; Thorkelson, 2000; Hunt *et al*., 2005; Fig. 21). The breccia bodies occur throughout the WSG but are most abundant in the lower part of the stratigraphy (Delaney, 1981; Lane, 1990) where there is a transition from metaevaporite-bearing calcareous metasedimentary rocks to overlying carbonaceous shale (Hunt *et al.*, 2005). Clasts within the breccia were locally derived from proximal host rocks and are generally sub-angular to sub-rounded,

ranging from < 1 cm to several hundred metres across. Early phases of Wernecke Breccia are preserved as clasts within later breccia. The breccia matrix is made up of rock fragments and hydrothermal precipitates consisting mainly of feldspar (albite and/or potassium feldspar), carbonate (calcite, or dolomite/ankerite, locally siderite) and quartz. IOCG mineralization comprises magnetite, hematite and chalcopyrite and lesser pitchblende, brannerite and cobaltite and occurs as multiple episodes of veining and disseminations within and peripheral to the breccia bodies (*cf.* Bell, 1986; Thorkelson, 2000; Hunt *et al.*, 2005).

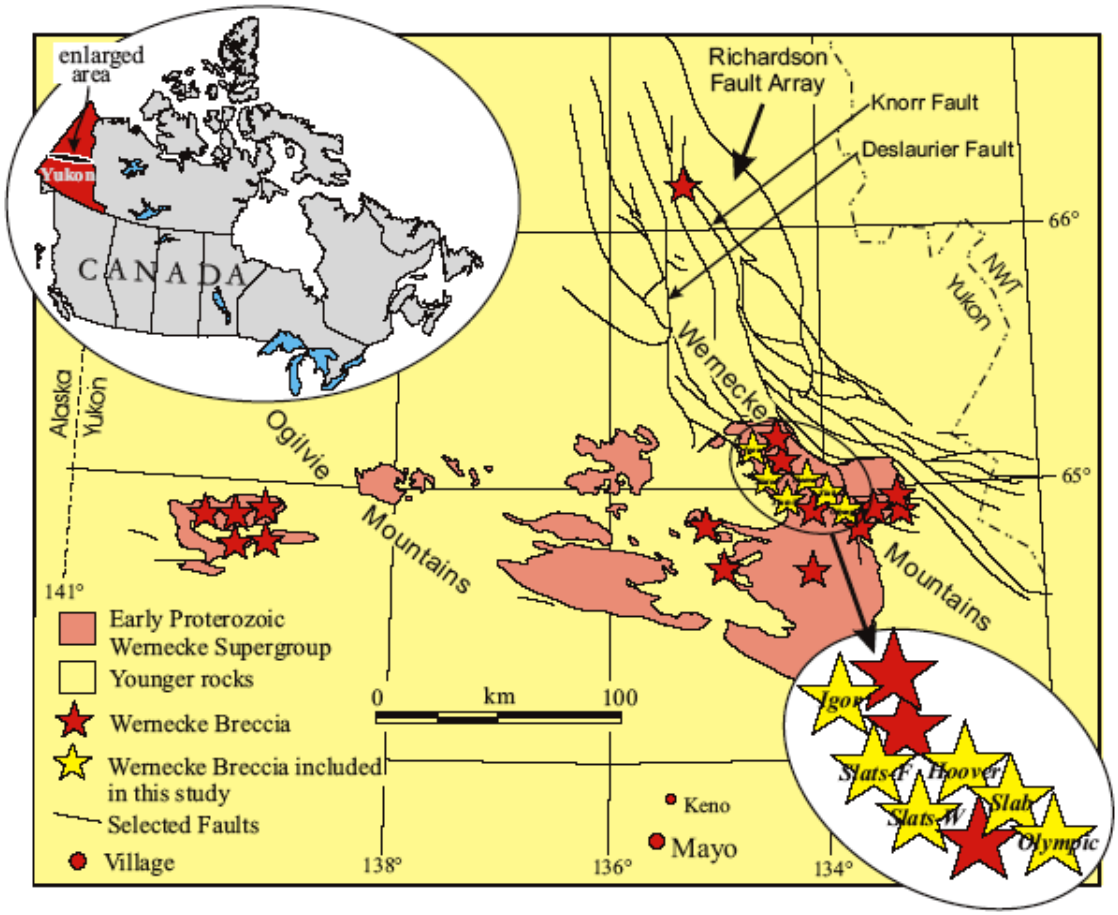

Figure 19: Regional setting of the Wernecke Breccia occurrences, Yukon, Canada (Hunt et al., 2005).

Brecciation and mineralization were associated with extensive metasomatic alteration that overprinted greenschist facies metamorphic assemblages in WSG (*cf.* Bell, 1986; Thorkelson, 2000; Brideau *et al.*, 2002; Hunt *et al.*, 2005). The alteration extends tens to hundreds of metres away from the breccia and varies in composition from sodic to potassic. Sodic alteration, typified by abundant albite and lesser scapolite (marialitic), is generally associated with breccia in metaevaporite-bearing (halite facies) WSG strata (Hunt *et al.*, 2005). Potassic alteration, characterised by abundant orthoclase ± sericite, is dominant in breccia hosted by clastic rocks in the remainder of WSG (Fig. 21). Sodic and potassic alteration assemblages are overprinted by widespread breccia-related carbonate alteration (calcite, dolomite, ankerite ± siderite).

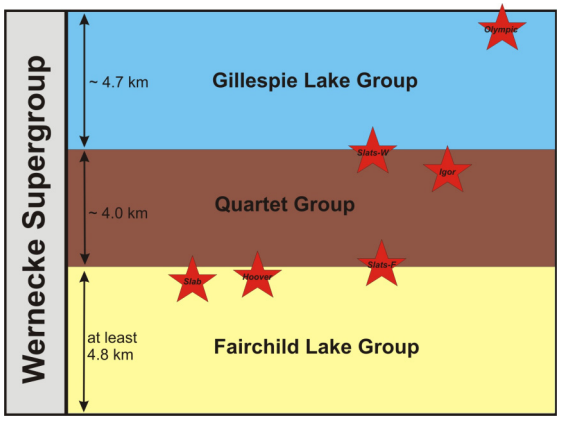

Figure 20: Stratigraphic setting of Wernecke breccia systems studied by Hunt et al. (2005).

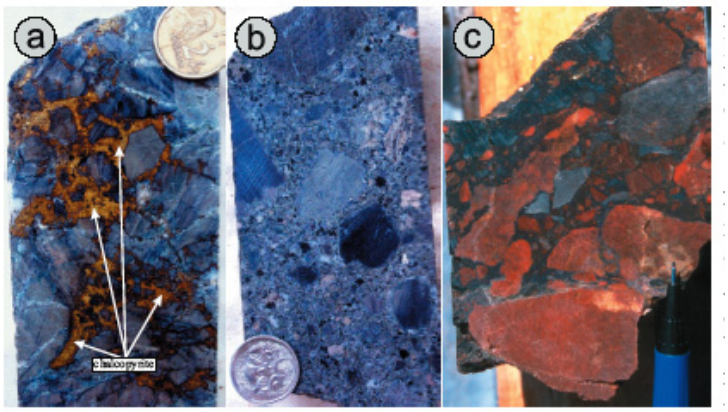

Figure 21: a. Chalcopyrite matrix with albitized WSG clasts; b. albite-altered breccia; c. K-feldspar altered breccia.

3.2 Fluid characteristics and chemistry

Microthermometry has been performed on fluid inclusions in selected quartz samples from the Igor, Slab, Hoover and Olympic prospects, Wernecke Mountains (Fig. 20). These samples were collected from quartz veins within and adjacent to breccia zones. The veins comprise quartz-carbonate (calcite, ankerite) with variable chalcopyrite ±pyrite ±magnetite ±hematite ±barite. The quartz contains both primary and secondary inclusions. The observed fluid inclusions are thought to represent syn- to post-brecciation fluids. Table 6 illustrates the fluid inclusion types observed at each of the deposits, along with a summary of the microthermometry results obtained from each location, and the proposed timing of the fluids, with respect to the breccia. The main inclusion types are type 3 two-phase aqueous inclusions (with 5 to 25% vapour; L+V), and type 2 halite-bearing inclusions (L+V+S). Eutectic (first) melting temperatures indicate the fluids are NaCl dominated, with the majority of samples containing significant calcium chloride content. Salinities calculated from ice melting and halite dissolution temperatures range between 3 and 40 wt % NaCl and homogenisation temperatures range from 70 to 261 °C.

Prospect	Type	Tfm (°C)	Major fluid components	Salinity (wt% NaCl equiv)	Th vap (°C)	Th hal (°C)	Th (°C)	Timing[2]
Slab	L+V+S	-61 to -54	H_2O NaCl, Ca, K, Mn	~40*	167 to 230	202 to 261	202 to 261	Syn
Hoover	L+V+S	-55 to -49	H_2O, NaCl, Ca, K	?*	152 to 200	?	>200	Syn
Igor	L+V	-56 to -38	H_2O, NaCl, Ca, K	30*	150 to 174	175 to 184	175 to 184	Syn-post
	L+V+S	-32 to -21	H2O, NaCl, Ca, K	3 to 23	70 to 138		70 to 138	
Olympic[1]	L+V & L+V+S		H_2O, NaCl, K, Ca	~30?	~200		~200	Post

Table 6: Thermometry data for fluid inclusions in quartz from four IOCG prospects in the Wernecke region. Tfm = first melting temperature. Th vap= temperature of vapour disappearance. Th hal = temperature of halite dissolution (where present). Th = final homogenization temperature. Major fluid compositions inferred by microthermometry and confirmed and complemented by PIXE analyses. * = salinity combined NaCl + $CaCl_2$. [1]Further data required at Olympic. [2]Timing is relative to the breccia.

PIXE analysis has been carried out on the two main types of inclusions and ongoing PhD research by David Gillen is currently evaluating the fluid chemistry in detail (Gillen et al., 2005). The Slab prospect

contains the most saline fluids, they are rich in calcium, and have the highest Ca/K ratios of all the deposits. An image of a halite-bearing (L+V+S) fluid inclusion from Slab is shown in Figure 22a, along with PIXE images of this inclusion. The images show the strong calcic nature of the fluids, and illustrates that significant components of Cl, Na, K, Mn and Fe are also present in the fluid. Figure 22b shows an inclusion and PIXE image from the Igor prospect. The Igor fluid inclusion has less intense signals for Cl, K and Ca. Bromine and chlorine ratios measured in fluid inclusions are consistent with fluids derived from bittern brines (Fig. 23).

A.

B.

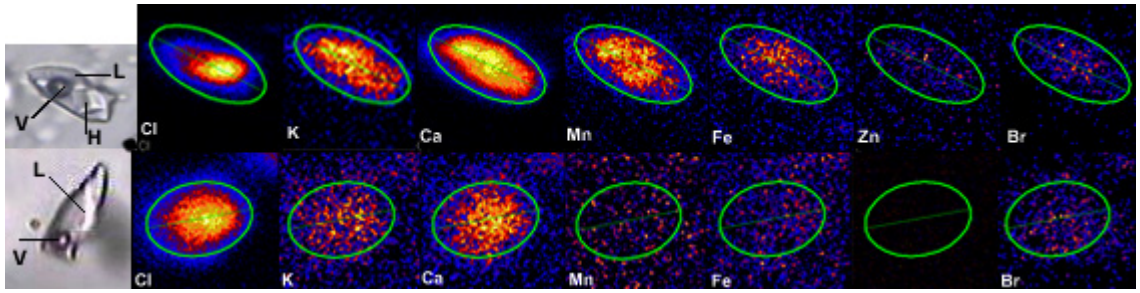

Figure 22: a. Type 2 inclusion from the Slab prospect and b. type 3 inclusion from the Igor prospect with PIXE images displaying the abundances of Cl, K, Ca, Mn, Fe, Zn, and Br within the fluid. Inclusion (a) is approx 20μm long, and (b) is approx 10μm. The location and intensity of the light coloured zones represent relative abundances of each element.

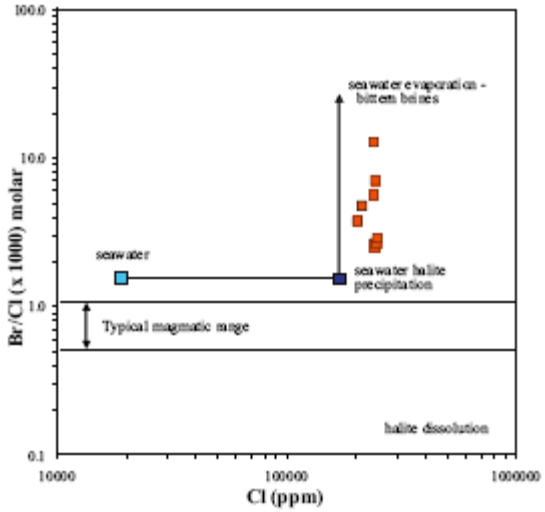

Figure 23: Br/Cl (x1000) mol ratio versus Cl (ppm) measured by PIXE in type 2 halite-bearing fluid inclusions from the Slab prospect. The data suggest that the fluids were derived from bittern brines similar to fluid inclusions in regional albitization from the Cloncurry district.

Oxygen and carbon isotopic compositions for breccia-related hydrothermal carbonate ($\delta^{18}O$ ≈ 9 to 20 ‰ SMOW; $\delta^{13}C$ ≈ -7 to +1 ‰ V-PDB) generally reflect those of host WSG strata ($\delta^{18}O_{limestone}$ ≈ 12 to 25 ‰; $\delta^{13}C_{limestone}$ ≈ -2 to +1 ‰; $\delta^{13}C_{carbonaceous\ shale}$ ≈ - 21 to -27 ‰). Sulfur isotopic compositions for hydrothermal pyrite, chalcopyrite and locally abundant barite ($\delta^{34}S_{pyrite\text{-}chalcopyrite}$ ≈ -12 to +13 ‰ CDT; $\delta\ ^{34}S_{barite}$ ≈ +8 to +17 ‰) point to a seawater (or sediments/evaporites deposited from seawater) source for sulfur (*ibid*). δNd values for Wernecke Breccia (δNd = -2.3 to -9.0) are similar to those for WSG strata (δNd_{1595} Ma = -3.5 to -8.4; Thorkelson *et al.*, 2005).

3.3 Noble Gas and Halogen Data from Step Heating Analysis for the Wernecke Breccias

Halogen step heating analysis of Wernecke samples exhibit a large range of Br/Cl and I/Cl values of between $0.4x10^{-3}$ to $2.9x10^{-3}$ and $0.3x10^{-6}$ to $46x10^{-6}$, respectively (Table 7). The majority of quartz samples have Br/Cl values that are lower than seawater and I/Cl values that are lower than the range determined for the magmatic fluids in Porphyry Copper Deposit (PCD) fluid inclusions and mantle diamond (Fig 1). The highest Br/Cl values were measured in sample DG10-1b and the fluorite plus barite samples. The highest Br/Cl and I/Cl values are higher than those measured in mineralization stage quartz veins selected from Mt Isa IOCG and are most similar to bittern brines (sedimentary formation waters). Together, the data points define a mixing array between a high Br/Cl and I/Cl bittern brine end-member and a Cl-rich end-member with Br/Cl $0.4x10^{-3}$ and I/Cl $x10^{-6}$. This mixing array is very similar to that observed for Mt Isa IOCG deposits but extend to slightly higher Br/Cl and I/Cl values (Kendrick et al., 2005; Fisher et al., 2006).

	Br/Cl $\times10^{-3}$ Range	I/Cl $\times10^{-6}$ Range	$^{40}Ar/^{36}Ar$ Mean-max	K/Cl Mean	Salinity Wt. % Mean	$^{40}Ar_E/Cl$ $\times10^{6}$ mean	$^{36}Ar/Cl$ $\times10^{-6}$ Max	$[^{40}Ar_E]\times10^{-3}$ cm^3cm^{-3} Mean	$[^{36}Ar]\times10^{-6}$ cm^3cm^{-3} Min.
Quartz samples (Stepped heating)									
DG96c	0.98-1.25	15.2-20.7	1261-2111	0.11	40	1.1×10^{-5}	160	1.4	1.0
DG10-1b	0.57-2.93	1.5-45.8	1582-5846	0.16	40	1.9×10^{-5}	100	3.0	1.6
STW	0.66-1.04	2.28-4.37	1347-2485	0.27	40	1.5×10^{-5}	131.2	2.4	1.2
Slab	0.37-1.89	0.3-11	1911-4722	0.23	40	1.2×10^{-5}	1500	1.8	0.2
OY94	0.80-1.06	4.0-17.2	6638-15,459	0.31	40	5.8×10^{-5}	178.5	9.0	0.8
Hoover	0.51-1.11	2.46-3.93	22,655-40,485	0.24	40	7.9×10^{-4}	302.8	122	0.6
						3.8×10^{-3}		588	
Barite and fluorite samples (In vacuo crushing)									
Igor barite	<2.6	<51.7	320-367	0.27	20	4.7×10^{-5}	1.3	3.6	59.5
Slats fluor	<2.8	<19.8	965-992	0.10	20	8.5×10^{-5}	9.3	6.5	8.2
Reference values									
meteoric			295	0	0	0		0	1.7
seawater	1.54	0.82	295		3.5				1.0

Table 7: Noble gas and halogen fluid compositions for Wernecke quartz, barite and fluorite samples.

The spread in the Br/Cl and I/Cl data is most easily explained by either 1) mixing between two crustal fluids, a bittern brine and halite dissolution water, or 2) by interaction of a single bittern brine with halite. Bittern brines are formed by the sub-aerial evaporation of seawater beyond the point of halite saturation. Halite saturated seawater has a salinity of 26-30 wt. % (Hanor, 1994). This value is lower than that of the most saline fluid inclusions in all of the samples, including those with a bittern brine signature (Table 7). Therefore, it is suggested that the salinities of >30 wt. % have been acquired by dissolution of halite at conditions of elevated pressure and temperature in the crust. If this is the case, the fluid end-member preserved in fluid inclusions with the bittern brine signature would originally have had even higher Br/Cl and I/Cl values, but a lower salinity. The minimum Br/Cl values of $0.4x10^{-3}$ are higher than those expected for pure halite dissolution water in which values of $0.1x10^{-3}$ are more typical (Fig 24). This can be explained if sylvite was significant within the evaporitic units dissolved by the mineralizing fluid because sylvite accommodates significantly more Br than halite. However, Br/Cl values of slightly greater than halite dissolution water are also expected if the fluid represents a bittern brine that has dissolved halite in the sub-surface. The entire range of Br/Cl and I/Cl values are most easily explained if halite was dissolved

by a bittern brine, with salinity of 26-30 wt % (or less if it was diluted by meteoric water) and starting Br/Cl and I/Cl values of greater than the highest measured values of $2.9x10^{-3}$ and $46x10^{-6}$.

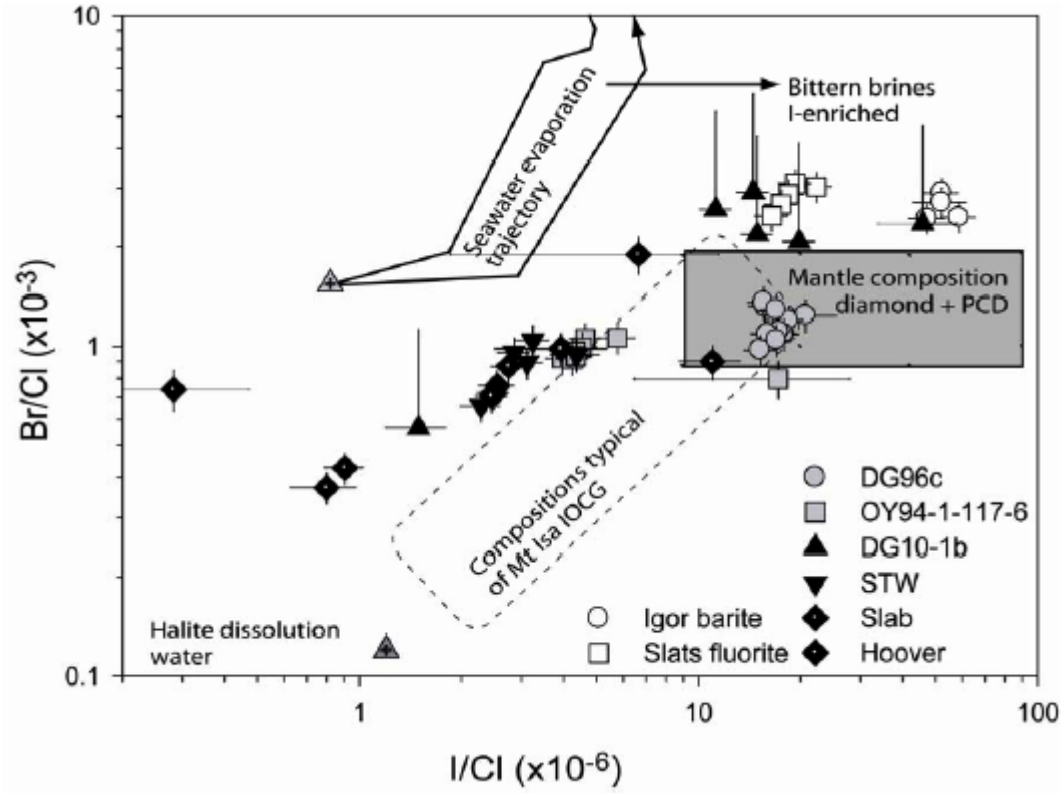

Figure 24: Br/Cl versus I/Cl for Wernecke IOCG prospects, Canada. Quartz data obtained by stepped heating uncrushed samples in the temperature range 200-700ºC. Barite and fluorite data obtained by in vacuo crushing. DG96c & DG10-1b from Igor; STW from Slats-Wallbanger; OY94-1-117-6 from Olympic prospect.

The minimum $^{40}Ar/^{36}Ar$ values determined for the Wernecke samples were measured in the barite and fluorite samples; barite has a $^{40}Ar/^{36}Ar$ value close to the modern day atmospheric value and fluorite has a $^{40}Ar/^{36}Ar$ value of <1000. Samples DG96c & DG10-1b from Igor, STW from Slats-Wallbanger and Slab have values of between 1000 and 6000. The highest values of 6600 - 40,400 were measured in samples from Olympic (OY94) and Hoover that have lower than mantle Br/Cl and I/Cl values (Fig. 24). Therefore, unlike the Ernest Henry deposit, the highest $^{40}Ar/^{36}Ar$ values are not correlated with the most mantle like Br/Cl and I/Cl values (Fig. 25). The calculated ^{36}Ar concentrations for the quartz samples are mainly lower than that of Air Saturated Water (ASW) but are much greater than ASW for the barite and fluorite samples (Table 7). The higher than ASW ^{36}Ar concentrations determined for the barite and fluorite may indicate that either the salinity of fluid inclusions in these samples is much lower than that used in Table 7 (ie <<20 wt %) or that these samples have been subjected to significant air contamination.

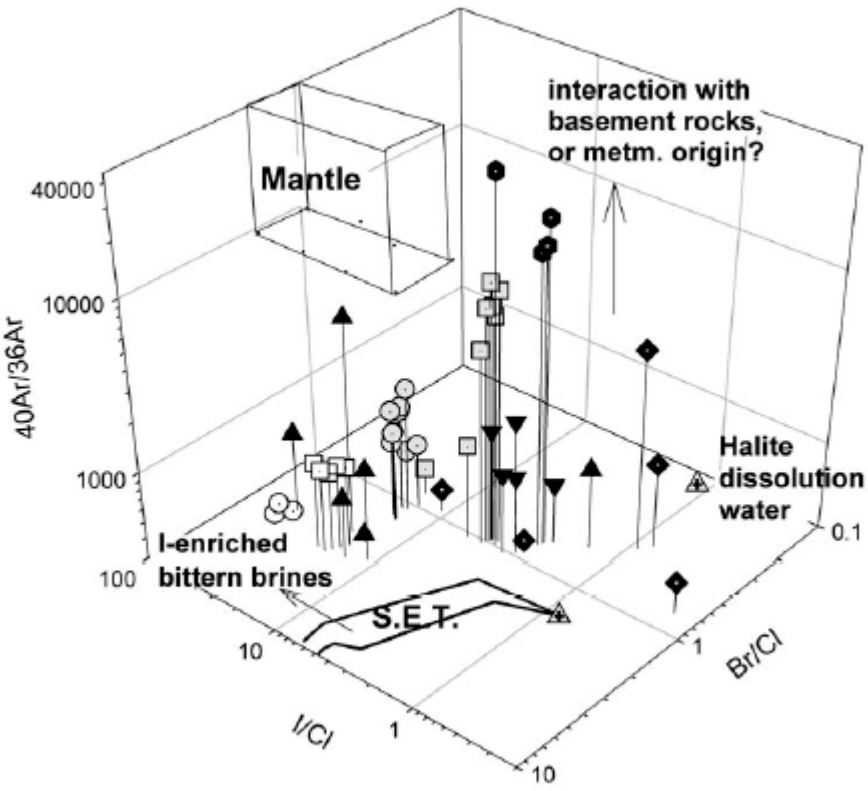

Figure 25: 3D log-log-log plot of Br/Cl vs I/Cl vs $^{40}Ar/^{36}Ar$ for Wernecke samples. Legend is as for Fig. 24. The seawater evaporation trajectory (SET) of Zherebstova and Volkova (1966), the composition of halite dissolution water involved in an MVT deposit (Bohlke and Irwin, 1992) and the box of mantle compositions based on diamond and PCD fluid inclusions (Johnson et al., 2000; Kendrick et al., 2001) are shown for reference.

The maximum $^{40}Ar/^{36}Ar$ value of 40,485 is within the range of values theoretically possible for metamorphic dehydration fluids and is only just above the value of 38,000 determined for brines with a probable metamorphic dehydration origin in the Mt Isa Copper deposit (Kendrick et al., 2006). A magmatic origin for the high $^{40}Ar/^{36}Ar$ value is less likely because the Wernecke breccias (1595 Ma) are ~100 million years younger than the BPRI (1710 Ma). Furthermore, in contrast to the Ernest Henry deposit with a maximum $^{40}Ar/^{36}Ar$ value of 29,000, the highest $^{40}Ar/^{36}Ar$ values are not found in samples with the most magmatic Br/Cl-I/Cl signatures (Fig 25). Nonetheless, the modern day MORB mantle has a $^{40}Ar/^{36}Ar$ value of 44,000 which based on model changes in the mantle $K/^{36}Ar$ corresponds to $^{40}Ar/^{36}Ar$ value of between 39,000 and 42,000 at 1.5 Ga (Kendrick et al., 2005). This implies that the geochemistry of the high $^{40}Ar/^{36}Ar$ fluid could be obtained by a magmatic fluid that had dissolved halite, a possibility in the Wernecke region whereby the BPRI may have intruded pre-existing halite sequences (e.g., Slab prospect).

3.4 Wernecke Breccia Genesis and Comparison with the Cloncurry District

Wernecke Breccia is spatially associated with faults on a regional and local scale (*cf.* Bell, 1986; Thorkelson, 2000) and breccia bodies were formed in weak and/or permeable regions during syn- to post-deformational expansion of over-pressured fluids (Thorkelson, 2000; Hunt *et al.*, 2005). The fluid inclusion and isotopic data above indicate the breccia-forming/mineralizing fluids were largely basinal in origin. The high salinity of the fluid and the Br/Cl data is consistent with derivation from an evaporite-bearing sedimentary sequence such as the WSG.

The difference in age between Wernecke Breccia (*ca*. 1595 Ma) and BPRI (*ca*. 1710 Ma) rules out a genetic link between the two (Thorkelson *et al.*, 2001a,b). The limited distribution of Slab volcanics, and cross-cutting relationships that demonstrate the volcanic rocks (undated) are older than (at least some phases of) breccia (Thorkelson, 2000; Laughton, 2004) indicate they are unlikely to be related to widespread brecciation. The coincidence of Wernecke Breccia and some BPRI (and Slab volcanics) may be a consequence of the use of similar fluid pathways. Some later dykes (*ca*. 1270 Ma) are also spatially coincident with BPRI and Wernecke Breccia suggesting similar fluid pathways were important for hundreds of millions of years. Alternatively, ductility contrasts between WSG sedimentary rocks and BPRI may have produced dilational zones during folding that focussed hydrothermal fluids and led to the preferential development of breccia in these sites.

The isotopic signature of fluids that formed Wernecke Breccia/IOCG mineralization and the lack of an obvious major intrusive heat source suggest fluid circulation and the high temperatures reached by the fluids occurred via mechanisms other than those related to magmatic heat flow. Fluid temperatures in at least the deeper part of the WSG would have been elevated due to the thickness of overlying sediments. A simple burial model using an average geothermal gradient of 25 ^{o}C would produce temperatures of 325 ^{o}C at depths of 13 km (estimated thickness of WSG). Breccia was formed syn- to post-deformation and fluid circulation could have been driven by tectonic, gravity and/or density processes (*cf.* Torgerson, 1990; Garven *et al.*, 2001). Another possible mechanism to provide high temperature fluids and drive circulation is via free convections cells whereby orogeny increases crustal permeability and causes the deep transitory circulation of fluids which allows the periodic release of heat (and possibly metals) from the crust (Deming, 1992). The above data therefore indicate the formation of Wernecke Breccia and associated IOCG mineralization may be related to the temporal evolution of the Wernecke basin independent of a magmatic cycle.

The Wernecke fluid inclusions are more akin to fluid inclusions found in the regional alteration systems in the Cloncurry district. There is a distinct absence of type 1 multisolid inclusions from the Wernecke region and type 2 and 3 inclusions are common with moderate homogenization temperatures and salinities, and Ca>K. Furthermore, Br/Cl ratios are high consistent with a bittern brine origin.

The noble gas and halogen data collected from the Wernecke IOCG prospects are similar to data from the Mt Isa IOCG deposits in only two respects. Namely the spread in Br/Cl and I/Cl values are compatible with the involvement of two or more fluid types in the ore mineralization process and the lowest values indicate the significant involvement of halite dissolution. In the Ernest Henry deposit of the Mt Isa Inlier, the involvement of two or more fluid end-members is favoured because the highest Br/Cl and I/Cl values are similar to the mantle and they preserve the highest $^{40}Ar/^{36}Ar$ values which is interpreted to favour the involvement of a magmatic fluid and cannot be explained by interaction of a single fluid with halite (Kendrick et al., 2005). The biggest difference between the Ernest Henry and the Wernecke data is that the high $^{40}Ar/^{36}Ar$ fluid at Wernecke has a lower than mantle halite dissolution Br/Cl-I/Cl signature and a magmatic fluid is a less likely fluid source at Wernecke.

4. Implications for the Genesis of IOCG Deposits

There is now mounting evidence to suggest that IOCG deposits formed from more than one fluid source and that fluid mixing was likely a major mechanism for ore formation (cf. Williams et al., 2001; Kendrick et al., 2005). There are several lines of evidence from the data presented here to support fluid mixing and different fluid sources including:

- Fluid inclusions in all the Cloncurry IOCG deposits that have been studied in detail display a very wide range in salinity and homogenization temperatures
- Different fluid inclusion types occur in the same paragenetic stage but there is an overall significant decrease in salinity through pre-, to syn- and post-ore stages.
- Major element ratios, particularly K/Ca, show wide variation within similar populations.
- Halogen data from two independent techniques (PIXE and step heating) indicate magmatic and evaporite (both bittern and halite-dissolution) derived salinity in IOCG deposits. Noble gas analysis also supports the involvement of surface derived fluid that has experienced crustal residence.

The relative contributions of these different fluids and their role in Cu transport is critical in evaluating barren to weakly mineralized environments versus ore systems (Fig. 26). The presence of the high temperature and ultra-high salinity type 1 fluid inclusions in the Cloncurry IOCG deposits suggests that these are key ingredients in ore formation. These inclusions are mostly absent from the barren regional alteration but present in the granite-hosted magmatic-hydrothermal systems. The Br/Cl ratios of type 1 inclusions within the deposits and granites are consistent with both a magmatic and halite dissolution salinity source with the latter potentially more dominant (see section 2.6). However, interestingly the highest Cu contents of type 1 inclusions have Br/Cl ratios consistent with a magmatic-derived source of salinity in both the IOCG and granite–hosted environments. This perhaps points towards a Cu-rich magmatic fluid pulse as being critical in forming significant ore deposits versus weakly mineralized regional systems. This idea is supported by noble gas data from Ernest Henry, the largest IOCG deposit in the region, that has the most mantle-like signature of the all the systems studied to date. Furthermore,

the barren regional alteration systems appear to lack a magmatic component and the salinity is mostly bittern derived.

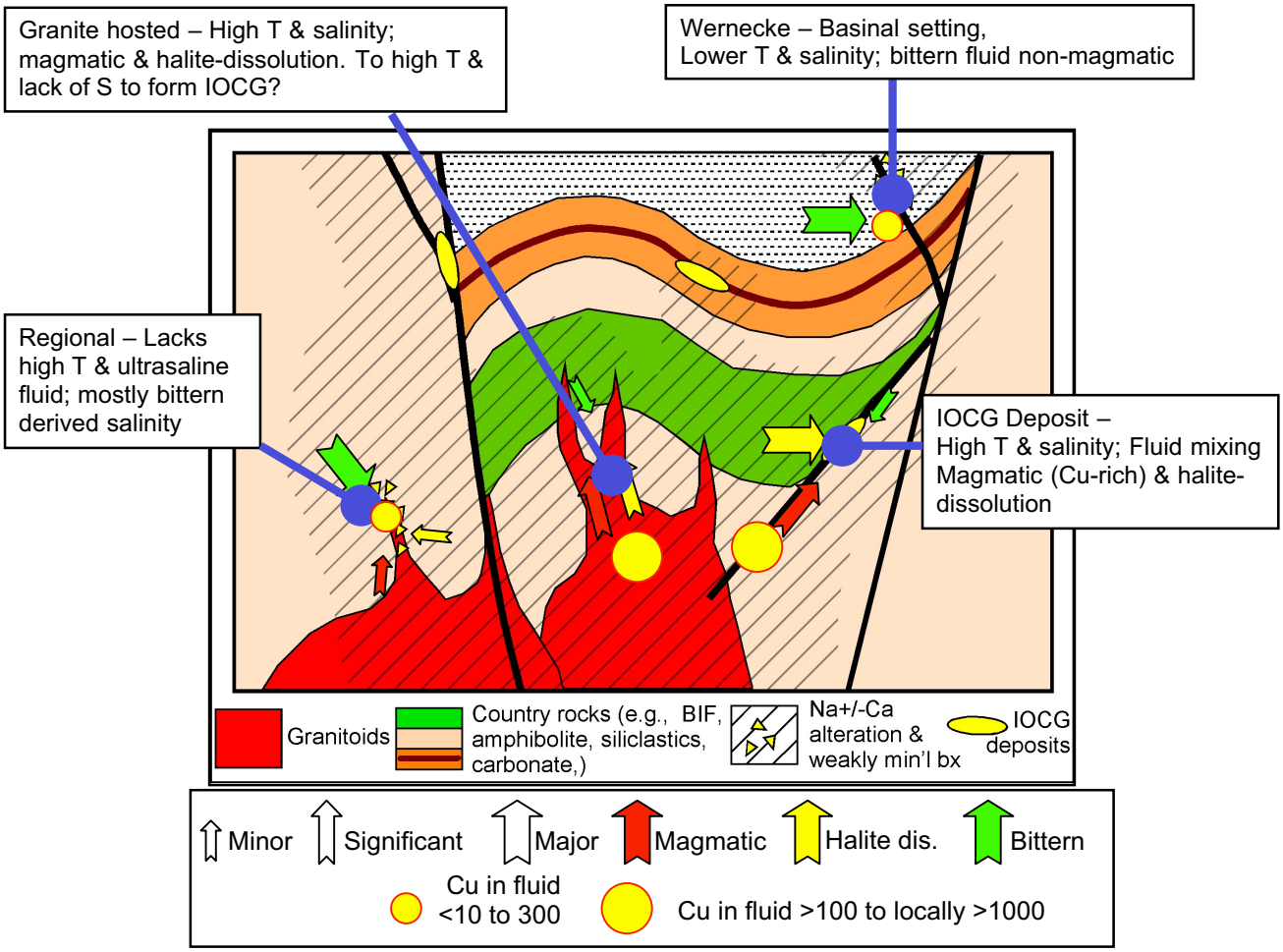

Figure 26: Model depicting fluid sources, conditions and chemistry in IOCG, granite and regional settings.

Non-magmatic evaporite-derived fluids are clearly capable of transporting Cu, however, the source rocks are not inherently Cu-enriched and, therefore, the fluids require interaction with Cu-bearing host rocks (e.g., mafic rocks). There is evidence for this in the Cloncurry district where saline brines have scavenged mafic rocks during albitization, although there is debate regarding the efficiency of this process (e.g., Williams, 1994; Oliver et al., 2004). Fluid inclusion results from the Wernecke breccia systems are compatible with fluid inclusions found in the regional alteration systems in the Cloncurry district both in terms of fluid inclusion types (mostly 2 and 3) and Br/Cl systematics (bittern derived). Copper mineralization in the Wernecke region is commonly associated with localized occurrences of mafic rocks and the most prospective region, Slab Mountain, contains the highest temperature and highest salinity fluids. It therefore seems likely that mineralization in Wernecke region formed from crustal brines that scavenged Cu from suitable host rocks but lacked any significant volatile magmatic input of salinity and importantly Cu.

The role of carbon dioxide is still poorly constrained. In several of the deposits CO_2-rich inclusions occur with type 1 multisolid inclusions that may represent fluid mixing or unmixing processes. Similar

relationships have been observed in granite-hosted environments and locally in regional systems. The carbon dioxide may play an important role in ore deposition by inducing phase separation at high temperature and pressure, and/or potentially transporting sulfur (e.g., Oliver et al., 2004). The latter, however, is still poorly constrained due to our inability to analyze sulfur in fluid inclusions. Sulfur is a critical ingredient in IOCG ore formation and there is evidence to suggest that some of the ultrasaline brines were sulfate poor due to the high Ba content (e.g., Williams et al., 2001). Sulfur isotope data from Cloncurry IOCG deposits ranges from -10 to +16 per mil, although many of the deposits have narrower ranges around 0 per mil (Williams and Pollard, 2003), suggesting a significant role for magmatic sulfur with an additional sedimentary contribution.

5. Ongoing Work and Recommended Further Work

Three PhD projects are continuing beyond the completion of the F3 project. Martina Bertelli will complete her work on fluids in barren regional breccia systems in the Cloncurry district during 2006. This work will include fluid inclusion studies and chemical modeling which will build upon her earlier studies of skarn systems (Bertelli et al., 2006). David Gillen will complete his work on fluids in the Wernecke breccias during 2006 which builds upon previous studies by Hunt et al. (2005). Louise Fisher is halfway through her PhD that is combining the expertise built up in the F3 project on Osborne and Starra with H4 halogen and noble gas research in order to further understand fluid and metal sources in IOCG deposits.

The research completed within F3 highlights significant gaps in our knowledge of IOCG regions, particularly in the Cloncurry district. A critical component of a mineral systems approach to exploration requires an understanding of potential source rocks and source fluids. Detailed fluid inclusion studies in and around granite environments is still lacking and needs to be addressed given the Cu-rich nature of some fluids in these environments. The source rocks for the evaporite-related fluids are poorly constrained in the Cloncurry district and there are no studies of fluid inclusions in potential source lithologies. The processes of fluid mixing are not well understood in terms of both physical mixing and chemical modeling; the high salinity nature of the fluids is particularly challenging for the latter. Carbon dioxide fluid inclusions are present in many systems but they have received relatively little attention compared to saline fluids. They likely have an important role in terms of fluid processes (e.g., immiscibility) and volatile transport (e.g., sulfur).

6. References

Adshead, N. D., 1995, Geology, Alteration and Geochemistry of the Osborne Cu-Au Deposit, Cloncurry District, N.W. Queensland, Australia.: Unpub. PhD thesis, James Cook University of North Queensland.

Adshead, N. D., Voulgaris, P., and Muscio, V. N., 1998, Osborne copper-gold deposit, in Berkman, D. A., and Mackenzie, D. H., eds., Geology of Australian and Papua New Guinean Mineral Deposits: Melbourne, The Australasian Institute of Mining and Metallurgy, p. 793-800.

Baker, T., 1998. Alteration, mineralization and fluid evolution at the Eloise Cu-Au deposit. Economic Geology, 93:1213-1233.

Baker, T., 2003. Annual pmd*CRC report July 2003: F3 Micrometallogeny of hydrothermal fluids. https://pmd-twiki.arrc.csiro.au/view/Pmdcrc/WebHome

Baker, T., Perkins, C., Blake, K.L., Williams, P.J., 2001. Radiogenic and stable isotope constraints on the genesis of the Eloise Cu-Au deposit, Cloncurry district, Australia. Economic Geology, 96:723-742.

Baker,T., Van Achterberg, E., Ryan, C.G., and Lang, J.R., 2004. Composition of ore fluids in a magmatic-hydrothermal skarn deposit. Geology, 32:117-120.

Barton, M.D., and Johnson, D.A., 1996, Evaporitic-source model for igneous-related Fe oxide-(REE-Cu-Au-U) mineralization: Geology v. 24, p. 259-262.

Beardsmore, T.J., 1992. Petrogenesis of Mount Dore-style breccia-hosted copper ± gold mineralization in the Kuridala-Selwyn region of Northwestern Queensland. Unpublished PhD thesis, James Cook University.

Bell, R.T., 1986, Megabreccias in northeastern Wernecke Mountains, Yukon Territory: Current Research, Part A, Geological Survey of Canada, Paper 86-1A, p. 375-384.

Bertelli, M., Baker, T., and Cleverley, J., 2006. Geochemical modeling of ore forming processes in skarn deposits, submitted to Chemical Geology.

Bertelli, M., Baker, T., and Cleverley, J., 2004. Controls on ore deposition in Zn-Pb skarns: geochemical modeling and fluid inclusion constraints. In Barnicoat, A.C., and Korsch, R.J., (eds.) Predictive Mineral Discovery Cooperative Research Centre – Extended Abstracts from the June 2004 Conference. Geocience Australia, Record 2004/9, p. 17-20.

Bodnar, R.J., 1995, Fluid inclusion evidence for a magmatic source of metals in porphyry copper deposits, in Thompson, J.F.H., ed., Magmas, fluid and ore deposits, Mineralogical Association Canada Short Course Series v. 23, p. 139-152.

Bohlke, J.K., and Irwin, J.J., 1992, Laser microprobe analyses of Cl, Br, I and K in fluid inclusions: implications for sources of salinity in some ancient hydrothermal systems: Geochimica et Cosmochimica Acta v. 56, p. 203-225.

Brideau, M-A., Thorkelson, D.J., Godin, L., and Laughton, J.R., 2002, Paleoproterozoic deformation of the Racklan Orogeny, Slats Creek (106D/16) and Fairchild Lake (106C/13) map areas, Wernecke Mountains, Yukon, in, Emond, D.S., Weston, L.H., and Lewis, L.L., eds., Yukon Exploration and Geology 2001, Exploration and Geological Services Division, Yukon Region, Indian and Northern Affairs Canada, p. 65-72.

Burnard P., Graham D., and Turner G. (1997) Vesicle-specific noble gas analyses of "popping rock"; implications for primordial noble gases in the Earth. Science 276, 568-571.

Delaney, G.D., 1981, The Mid-Proterozoic Wernecke Supergroup, Wernecke Mountains, Yukon Territory, in, Proterozoic Basins of Canada, Geological Survey of Canada, Paper 81-10, p. 1-23.

Deming, D., 1992, Catastrophic release of heat and fluid flow in the continental crust: Geology v. 20, p. 83-86.

De Jong, G. and Williams, P.J. 1995. Evolution of metasomatic features during exhumation of mid crustal Proterozoic rocks in the vicinity of the Cloncurry Fault, NW Queensland. Australian Journal of Earth Sciences , v.42, p. 281-290.

Fisher, L., 2005. Fluid inclusion compositions and conditions at Osborne; preliminary results. https://pmd-twiki.arrc.csiro.au/view/Pmdcrc/WebHome

Fu, B., Baker, T., Oliver, N.H.S., Williams, P.J., Ulrich, T., Mernagh, T.P., van Achterberg, E., Ryan, C.G., Marshall, L.J., Rubenach, M.J., Mark, G., Yardley, B.W.D., 2004a. Regional fluid compositions of the Mount Isa Eastern Succession, NW Queensland, Australia. In Barnicoat, A.C., and Korsch, R.J., (eds.) Predictive Mineral Discovery Cooperative Research Centre – Extended Abstracts from the June 2004 Conference. Geocience Australia, Record 2004/9, p. 63-66.

Fu, B., Oliver, N.H.S., Baker, T., Williams, P.J., Marshall, L.J., Rubenach, M.J., Ulrich, T., van Achterberg, E., Ryan, C.G., and Yardley, B.W.D., 2004b. Microanalysis of regional fluids from the Eastern Succession of the Mount Isa Block, NW Queensland. In J. Muhling et al. (eds) SEG 2004: Predictive

Mineral Discovery Under Cover; Extended Abstracts. Centre for Global Metallogeny, The University of Weestern Australia, Publication No. 33, p. 378-382.

Garven, G., Bull., S.W., and Large, R.R., 2001, Hydrothermal fluid flow models of stratiform ore genesis in the McArthur Basin, Northern Territory, Australia: Geofluids v. 1, p. 289-311.

Gauthier L., Hall G., Stein H., Schaltegger U., 2001, The Osborne Deposit, Cloncurry District: A 1595 Ma Cu-Au Skarn Deposit. In A Hydrothermal Odyssey, 43 Extended conference Abstracts, Ed. Williams P.J., James Cook University, Townsville, pp 58-59.

Gillen, D., Baker, T., Hunt, J., Ryan, C., Win, T.T., and Ulrich, T., 2005. PIXE and LAICPMS analysis of IOCG related hydrothermal fluids in the Wernecke Mountains, Canada. In Structure, tectonics and ore mineralization processes, abstract volume, Ed. Hancock, H., et al., EGRU Contribution 64, p. 173.

Gillen, D., Baker, T., Hunt, J., Ryan, C., and Win, T.T., 2004. PIXE analysis of hydrothermal fluids in the Wernecke Mountains, Canada. In Barnicoat, A.C., and Korsch, R.J., (eds.) Predictive Mineral Discovery Cooperative Research Centre – Extended Abstracts from the June 2004 Conference. Geocience Australia, Record 2004/9, p. 69-74.

Hitzman, M.W., Oreskes, N., and Einaudi, M.T., 1992, Geological characteristics and tectonic setting of Proterozoic iron oxide (Cu-U-Au-REE) deposits: Precambrian Research, v. 58, p. 241-287.

Hunt, J., Baker, T., and Thorkelson, D., 2005. Regional-scale Proterozoic IOCG-mineralized breccia systems: examples from the Wernecke Mountains, Yukon, Canada. Mineralium Deposita, 40:492-514

Johnson L.H., Burgess R., Turner G., Milledge H.J., and Harris J.W., 2000, Noble gas and halogen geochemistry of mantle diamonds: Comparison of African and Canadian diamonds. Geochim. Cosmochim. Acta 64, 717-732.

Kendrick, M. A., Burgess, R., Pattrick, R. A. D., and Turner, G., 2001, Fluid inclusion noble gas and halogen evidence on the origin of Cu-Porphyry mineralising fluids.: Geochimica et Cosmochimica Acta, v. 65, p. 2651-2668.

Kendrick, M. A., Mark, G., and Phillips, D., 2005. A tale of three fluids: noble gas and halogen evidence on the origin of the giant Ernest Henry IOCG deposit, Australia. https://pmd-twiki.arrc.csiro.au/view/Pmdcrc/WebHome

Lane, R.A., 1990, Geologic setting and petrology of the Proterozoic Ogilvie Mountains breccia of the Coal Creek Inlier, southern Ogilvie Mountains, Yukon Territory [MSc. Thesis] University of British Columbia, Vancouver, British Columbia, Canada, 223p.

Laughton, J.R., 2004, The Proterozoic Slab volcanics of northern Yukon, Canada: megaclasts of a volcanic succession in Proterozoic Wernecke Breccia, and implications for the evolution of northwestern Laurentia [PhD Thesis] Simon Fraser University, Burnaby, British Columbia, Canada, 200p.

Mark,G., Baker, T., Williams, P.J., Mustard, R., Ryan, C., and Mernagh, T.P., 2004. The geochemistry of magmatic fluids, Cloncurry district, Australia: relations to IOCG systems. In Barnicoat, A.C., and Korsch, R.J., (eds.) Predictive Mineral Discovery Cooperative Research Centre – Extended Abstracts from the June 2004 Conference. Geocience Australia, Record 2004/9, p. 123-126.

Mark G., and Foster D.R.W., 2000, Magmatic albite-actinolite-apatite-rich rocks from Cloncurry district, Northwest Queensland, Australia. Lithos 51, 223-245.

Mustard, R., Baker, T., Williams, P. J., Mernagh, T. P., Ryan, C. G., Van Achterberg, E., and Adshead, N. D., 2004, The role of unmixing in magnetite ± copper deposition in Fe-oxide Cu-Au systems In Barnicoat, A.C., and Korsch, R.J., (eds.) Predictive Mineral Discovery Cooperative Research Centre – Extended Abstracts from the June 2004 Conference. Geocience Australia, Record 2004/9, p. 155-160.

Mustard, R., Mark, G., Ulrich, T., Foster, D., and Gillen, D., 2005. Geochemsitry of magmatic fluids from intrusions in the Williams-Naraku batholith, Cloncurry district, NW Queensland: preliminary results from laser ablation ICPMS analysis. https://pmd-twiki.arrc.csiro.au/view/Pmdcrc/WebHome

Oliver, N.H.S., Cleverley, J.S., Mark, G., Pollard, P.J., Fu, B., Marshall, L.J., Rubenach, M.J., Williams, P.J., and Baker, T., 2004. Modeling the role of sodic alteration in the genesis of iron oxide-copper-gold deposits, eastern Mount Isa Block, Australia. Economic Geology 99: 1145-1176.

Perkins, C. and Wyborn, L., 1998. Age of Cu-Au mineralization, Cloncurry district, eastern Mount Isa Inlier, Queensland, as determined by $^{40}Ar/^{39}Ar$ dating. Australian Journal of Earth Sciences, v45, pp233-246.

Perring, C.S., Pollard, P.J., Dong, G., Nunn, A.J., and Blake, K.L., 2000, The Lightening Creek sill complex, Cloncurry district, northwest Queensland: a source of fluids for Fe oxide Cu-Au mineralization and sodic-calcic alteration: Economic Geology, v. 95, p. 1067-1090.

Pollard, P.J., 2001, Sodic(-calcic) alteration in Fe oxide-Cu-Au districts: an origin via unmixing of magmatic-derived H_2O-CO_2-NaCl±$CaCl_2$-KCl fluids: Mineralium Deposita, v. 36, p.93-100.

Pollard, P.J., 2000, Evidence of a magmatic fluid and metal source for Fe oxide Cu-Au mineralisation. in Porter, T.M., ed., Hydrothermal Iron Oxide Copper-Gold & Related Deposits: A Global Perspective, volume 1: PGC Publishing, Adelaide, p. 27-41.

Rotherham, J.F., 1997. A metasomatic origin for the iron oxide-Au-Cu Starra orebodies, Eastern Fold Belt, Mount Isa Inlier. Mineralium Deposita, v32, pp205-218.

Rotherham, J.F., Blake, K.L., Cartwright I. and Williams, P.J., 1998. Stable isotope evidence for the origin of the Mesoprooterozoic Starra Au-Cu deposit, Cloncurry district, northwest Queensland. Economic Geology, v93, pp1435-1449.

Rubenach, M.J., Adshead, N. Oliver, N., Tullemans, F., Esser, D., and Stein, H., 2001. The Osborne Cu-Au deposit – Geochronology and genesis of mineralization in relation to host albitites and ironstones. EGRU Contribution 59:173-173.

Thorkelson, D.J., 2000, Geology and mineral occurrences of the Slats Creek, Fairchild Lake and "Dolores Creek" areas, Wernecke Mountains, Yukon Territory: Exploration and Geological Services Division, Yukon Region, Indian and Northern Affairs Canada, Bulletin 10, 73p.

Thorkelson, D.J., Mortensen, J.K., Creaser, R.A., Davidson, G.J., and Abbott, J.G., 2001a, Early Proterozoic magmatism in Yukon, Canada: constraints on the evolution of northwestern Laurentia: Canadian Journal of Earth Science, v. 38, p.1479-1494.

Thorkelson, D.J., Mortensen, J.K., Davidson, G.J., Creaser, R.A., Perez, W.A., and Abbott, J.G., 2001b, Early Mesoproterozoic intrusive breccias in Yukon, Canada: The role of hydrothermal systems in reconstructions of North America and Australia: Precambrian Research, v. 111, p. 31-55Torgerson, 1990

Torgersen, T., 1990, Crustal-scale fluid transport, magnitude and mechanisms: EOS (Transactions, American Geophysical Union), v. 71, p. 1,4,13.

Whitney, J.A., Hemley, J.J., and Simon, F.O., 1985, The concentration of iron in chloride solutions equilibrated with synthetic granite compositions: the sulfur-free system, Economic Geology, v. 80, p. 444-460

Williams P.J., 1994. Iron mobility during synmetamorphic alteration in the Selwyn Range area, NW Queensland: implications for the origin of ironstone-hosted Au-Cu deposits. Mineralium Deposita, v29, pp250-260

Williams, P.J., Dong, G., Ryan, C.G., Pollard, P.J., Rotherham, J.F., Mernagh, T.P., and Chapman, L.H., 2001, Geochemistry of hypersaline fluid inclusions from the Starra (Fe oxide)-Au-Cu deposit, Cloncurry district, Queensland, Economic Geology, v. 96, p. 875-884.

Williams, P.J., Baker, T., Ulrich, T., and Ryan, C.G., 2004a. Fluid inclusion microanalysis: advances and future challenges. In Barnicoat, A.C., and Korsch, R.J., (eds.) Predictive Mineral Discovery Cooperative Research Centre – Extended Abstracts from the June 2004 Conference. Geocience Australia, Record 2004/9, p. 229-232.

Williams, P.J., Broman, C., Dong, G., Mark, G., Martinsson, O., Mernagh, T., Pollard, P.J., Ryan, C.G., and Win, T.T., 2004b. PIXE characterization of fluid inclusion brines from Proterozoic Fe oxide-bearing Cu-Au Deposits, Norrbotten (Sweden) and the Cloncurry District (NW Queensland). Mineralium Deposita, in review.

Williams, P.J., Dong, G., Yardley, B.W.D., Ulrich, T., Ryan, C., and Mernagh, T., 2005. Lead and zinc-rich fluid inclusions in Broken Hill-type deposits: fractionates from sulphide-rich melys or consequences of exotic fluid infiltration? In Mineral deposit research: meeting the global challenge, Eds. Mao, J., and Bierlien, F.P., Proceeding of the 8th Biennial SGA Meeting Beijing, vol. 1, chapt. 7.36, p. 861-864.

Williams, PJ, and Pollard, PJ, 2003. Australian Proterozoic iron oxide-copper-gold deposits: an overview with new metallogenic and exploration data from the Cloncurry district NW Queensland, Exploration and Mining Geology v. 10, No. 3, p. 1-23.

Xu, G., 2000, Fluid inclusions with NaCl-CaCl2-H2O composition from the Cloncurry hydrothermal system, NW Queensland, Australia: Lithos, v.53, p. 21-35.

Zherebtsova I.K. and Volkova N.N., 1966, Experimental study of behaviour of trace elements in the process of natural solar evaporation of Black Sea water and Lake Sasky-Sivash brine. Geochem. Int. 3, 656-670

7. Digital Appendix

F3 Final Report Powerpoint Presentation

F3 Related Journal Papers

Baker,T., Van Achterberg, E., Ryan, C.G., and Lang, J.R., 2004. Composition of ore fluids in a magmatic-hydrothermal skarn deposit. Geology, 32:117-120.

Hunt, J., Baker, T., and Thorkelson, D., 2005. Regional-scale Proterozoic IOCG-mineralized breccia systems: examples from the Wernecke Mountains, Yukon, Canada. Mineralium Deposita, 40:492-514

F3 Related Extended Conference Abstracts

Bertelli, M., Baker, T., and Cleverley, J., 2004. Controls on ore deposition in Zn-Pb skarns: geochemical modeling and fluid inclusion constraints. In Barnicoat, A.C., and Korsch, R.J., (eds.) Predictive Mineral Discovery Cooperative Research Centre – Extended Abstracts from the June 2004 Conference. Geocience Australia, Record 2004/9, p. 17-20.

Fu, B., Baker, T., Oliver, N.H.S., Williams, P.J., Ulrich, T., Mernagh, T.P., van Achterberg, E., Ryan, C.G., Marshall, L.J., Rubenach, M.J., Mark, G., Yardley, B.W.D., 2004a. Regional fluid compositions of the Mount Isa Eastern Succession, NW Queensland, Australia. In Barnicoat, A.C., and Korsch, R.J., (eds.) Predictive Mineral Discovery Cooperative Research Centre – Extended Abstracts from the June 2004 Conference. Geocience Australia, Record 2004/9, p. 63-66.

Fu, B., Oliver, N.H.S., Baker, T., Williams, P.J., Marshall, L.J., Rubenach, M.J., Ulrich, T., van Achterberg, E., Ryan, C.G., and Yardley, B.W.D., 2004b. Microanalysis of regional fluids from the Eastern Succession of the Mount Isa Block, NW Queensland. In J. Muhling et al. (eds) SEG 2004: Predictive Mineral Discovery Under Cover; Extended Abstracts.

Gillen, D., Baker, T., Hunt, J., Ryan, C., and Win, T.T., 2004. PIXE analysis of hydrothermal fluids in the Wernecke Mountains, Canada. In Barnicoat, A.C., and Korsch, R.J., (eds.) Predictive Mineral Discovery Cooperative Research Centre – Extended Abstracts from the June 2004 Conference. Geocience Australia, Record 2004/9, p. 69-74.

Mark,G., Baker, T., Williams, P.J., Mustard, R., Ryan, C., and Mernagh, T.P., 2004. The geochemistry of magmatic fluids, Cloncurry district, Australia: relations to IOCG systems. In Barnicoat, A.C., and Korsch, R.J., (eds.) Predictive Mineral Discovery Cooperative Research Centre – Extended Abstracts from the June 2004 Conference. Geocience Australia, Record 2004/9, p. 123-126.

Mustard, R., Baker, T., Williams, P. J., Mernagh, T. P., Ryan, C. G., Van Achterberg, E., and Adshead, N. D., 2004, The role of unmixing in magnetite ± copper deposition in Fe-oxide Cu-Au systems: Predictive Mineral Discovery Research Centre - Extended Abstracts from the June 2004 Conference, Barossa Valley, 2004.

Williams, P.J., Baker, T., Ulrich, T., and Ryan, C.G., 2004a. Fluid inclusion microanalysis: advances and future challenges. In Barnicoat, A.C., and Korsch, R.J., (eds.) Predictive Mineral Discovery Cooperative Research Centre – Extended Abstracts from the June 2004 Conference. Geocience Australia, Record 2004/9, p. 229-232.

Williams, P.J., Dong, G., Yardley, B.W.D., Ulrich, T., Ryan, C., and Mernagh, T., 2005. Lead and zinc-rich fluid inclusions in Broken Hill-type deposits: fractionates from sulphide-rich melys or consequences of exotic fluid infiltration? In Mineral deposit research: meeting the global challenge, Eds. Mao, J., and Bierlien, F.P., Proceeding of the 8th Biennial SGA Meeting Beijing, vol. 1, chapt. 7.36, p. 861-864.

F3 Related pmd*CRC Reports 2005

Fisher, L., 2005. Fluid inclusion compositions and conditions at Osborne; preliminary results.

Mustard, R., Mark, G., Ulrich, T., Foster, D., and Gillen, D., 2005. Geochemsitry of magmatic fluids from intrusions in the Williams-Naraku batholith, Cloncurry district, NW Queensland: preliminary results from laser ablation ICPMS analysis.

Bertelli, M., Baker, T., and Cleverley, J., 2006. Geochemical modeling of ore forming processes in skarn deposits.

F3 Quarterly Reports 2002-05

June 2002
September 2002
December 2002

March 2003
June 2003
September 2003
December 2003

March 2004
June 2004
September 2004
December 2004

March 2005
June 2005